

# A Hippo Pathway-Related GCK Controls Both Sexual and Vegetative Developmental Processes in the Fungus *Sordaria macrospora*

Daria Radchenko,\* Ines Teichert,\* Stefanie Pöggeler,<sup>†</sup> and Ulrich Kück\*<sup>1</sup>

\*Lehrstuhl für Allgemeine und Molekulare Botanik, Ruhr-Universität Bochum, 44780, Germany and <sup>†</sup>Genetik Eukaryotischer Mikroorganismen, Institut für Mikrobiologie und Genetik, Universität Göttingen, 37077, Germany

ORCID IDs: 0000-0002-2993-6756 (I.T.); 0000-0002-6842-4489 (S.P.)

**ABSTRACT** The supramolecular striatin-interacting phosphatases and kinases (STRIPAK) complex is conserved from yeast to human, and regulates a variety of key biological processes. In animals, this complex consists of the scaffold protein striatin, the protein phosphatase 2A, and kinases, such as germinal center kinase (GCK) III and GCKIV family members, as well as other associated proteins. The STRIPAK complex was identified as a negative regulator of the Hippo pathway, a large eukaryotic signaling network with a core composed of a GCK and a nuclear Dbf2-related kinase. The signaling architecture of the Hippo core resembles the fungal septation initiation network (SIN) that regulates cytokinesis in fission yeast as well as septation in filamentous fungi. In the filamentous model fungus *Sordaria macrospora*, core components of the STRIPAK complex have been functionally described and the striatin homolog PRO11 has been shown to interact with the GCK SmKIN3. However, the exact role of SmKIN3 in fungal development has not yet been fully elucidated. Here, we provide comprehensive genetic and functional analysis of SmKIN3 from *S. macrospora*. Using deletion mutants and site-directed mutagenesis, along with phenotypic and phylogenetic analysis, we provide compelling evidence that SmKIN3 is involved in fruiting body formation, hyphal fusion, and septation. Strains carrying the ATP-binding mutant SmKIN3<sup>K39R</sup>, as well as a double-deletion strain lacking SmKIN3 and the core STRIPAK subunit PRO11, also revealed severe developmental defects. Collectively, this study suggests that SmKIN3 links both the SIN and STRIPAK complex, thereby regulating multiple key cellular processes.

**KEYWORDS** germinal center kinase; septation; fungal sexual development; STRIPAK; Hippo pathway; *Sordaria macrospora*

**G**ERMINAL center kinases (GCKs) are Ste20-related serine/threonine kinases (STKs) with a conserved catalytic domain located at the N-terminus. In mammals, flies, and worms, eight GCK subfamilies (I–VIII) are known, and are distinguished according to their structure and biological function (Delpire 2009). Some members of these subfamilies transmit extracellular signals to mitogen-activated protein kinase (MAPK) cascades, while others act as signaling hubs

within conserved eukaryotic complexes. Five out of eight GCK subfamilies (GCK-I, II, III, IV, and VIII) were shown to functionally interact with either the Hippo pathway, the supramolecular striatin-interacting phosphatases and kinases (STRIPAK) complex, or with both (Couzens *et al.* 2013; Madsen *et al.* 2015; Meng *et al.* 2015, 2016; Thompson and Sahai 2015). GCKs regulate key developmental processes, such as cytoskeleton organization, the cell cycle, and apoptosis. In humans, malfunction of GCKs is associated with different medical conditions, including autoimmune diseases and cancer, which highlights them as potential therapeutic targets (Delpire 2009; Yin *et al.* 2012; Thompson and Sahai 2015).

The STRIPAK complex is highly conserved in eukaryotes, and its core consists of the protein phosphatase 2A (PP2A) B<sup>56</sup>-regulatory subunit striatin, the scaffold and catalytic subunits PP2AA and PP2AC, the striatin-interacting protein STRIP1/2, the monopolar spindle one-binder (Mob) protein

Copyright © 2018 by the Genetics Society of America

doi: <https://doi.org/10.1534/genetics.118.301261>

Manuscript received April 25, 2018; accepted for publication June 25, 2018; published Early Online July 16, 2018.

Available freely online through the author-supported open access option.

Supplemental material available at Figshare: <https://doi.org/10.25386/genetics.6741290>.

<sup>1</sup>Corresponding author: Lehrstuhl für Allgemeine und Molekulare Botanik, Ruhr-Universität Bochum, Universitätsstr. 150, ND 7/130, 44780 Bochum, Germany. E-mail: [ulrich.kueck@rub.de](mailto:ulrich.kueck@rub.de)

Mob3, and—in vertebrates and invertebrates—the cerebral cavernous malformation 3 (CCM3) protein. In mammals, additional proteins, such as the sarcolemmal membrane-associated protein (SLMAP), the suppressor of IKK $\epsilon$ , and the fibroblast growth factor receptor oncogene partner 2, or the cortactin-binding protein 2, can interact with the core STRIPAK in a mutually exclusive manner. Moreover, it is highly likely that STRIPAK-association of GCK-III and GCK-IV family kinases is also mutually exclusive. GCK-III kinases mammalian Ste20-like (MST) 3 (STK24), MST4 (STK26; MASK), and YSK1 (STK25; SOK1) bind to striatin family members via CCM3. However, whether GCK-IV kinases Misshapen (Msn)-like kinase 1 (MINK1; MAP4K6) and MAP4K4 interact with striatin directly or via CCM3 is as yet not completely understood (Hwang and Pallas 2014). Finally, GCK-III kinases are thought to be downregulated by PP2A (Gordon *et al.* 2011).

*Drosophila melanogaster* possesses only one homolog of each of the mammalian GCK families, thereby indicating partial redundancy of vertebrate GCKs. GCK-III kinase Wheezy (GckIII) and GCK-IV kinase Misshapen (Msn) were found in affinity capture-mass spectrometry with the striatin homolog Cka and the MOB3 homolog Mob4, confirming these factors to be a part of the dSTRIPAK complex (Ribeiro *et al.* 2010). Interestingly, *D. melanogaster* Msn and GCK-I kinase Happy-hour (Hppy) were shown as alternative activators of the nuclear Dbf2-related (NDR) kinase Warts of the Hippo pathway (Li *et al.* 2015; Zheng *et al.* 2015), and the same conclusion was drawn for the human homologs MINK1, MAP4K4, and MAP4K1/2/3/5 (Meng *et al.* 2015).

The Hippo pathway in *D. melanogaster*, as well as its human counterpart, represent large signaling networks. Its core consists of GCK-II kinase Hippo (MST1/2 in human, also known as STK4/3) associated with the adaptor protein Salvador (SAV1 in human), and the NDR kinase Warts (large tumor suppressor1/2 or LATS1/2 in human) associated with the kinase activator Mob1 (MOB1). Of note is that malfunction of the Hippo pathway leads to tissue overgrowth and tumor formation (Pan 2007, 2010). In particular, lack of MST1/2 in mammalian cells is connected with the development of carcinoma, adenoma, and acute leukemia (Pan 2010; Harvey *et al.* 2013; Richardson and Portela 2017). GCK-II kinases interact with STRIPAK by binding via their C-terminal linker to a forkhead-associated domain of SLMAP, thereby enabling their dephosphorylation by PP2AC. At the same time, SAV1 inhibits the phosphatase activity of PP2A via binding to the STRIPAK core, thus disabling dephosphorylation of the GCKII activation-loop. This mechanism is responsible for the reciprocal downregulation of STRIPAK and Hippo (Couzens *et al.* 2013; Bae *et al.* 2017). Even though Hippo kinases MST1 and MST2 are capable of autophosphorylation-dependent activation, they can also be activated by an upstream regulator, namely GCK-VIII kinases TAO1/2/3 (Fallahi *et al.* 2016; Meng *et al.* 2016). Collectively, these facts provide evidence for a complex GCK signaling network.

Although animal GCKs have been extensively investigated, their evolutionary history remains unclear (Sebé-Pedrós *et al.*

2012, 2016). Molecular mechanisms, underlying multiple GCK-related disease phenotypes in mammals, also require further investigation (Maugeri-Saccà and De Maria 2018; Xiang *et al.* 2018). Moreover, new GCK targets, regulators, and interaction partners are being steadily identified (Johnson and Halder 2014; Meng *et al.* 2016).

Interestingly, signaling pathways from metazoans share more similarities with those from fungi, rather than with those from plants or protists. Indeed, fungal model organisms have been highly helpful in advancing our understanding of conserved eukaryotic signaling pathways in general, and the structure and function of these conserved pathways in particular (Glotzer 2017). The animal Hippo pathway, which resembles the septation initiation network (SIN) from *Schizosaccharomyces pombe*, is a prominent example. Both, the Hippo and the SIN are kinase cascades, which have a core consisting of a highly conserved GCK and an NDR kinase. In yeast, SIN is required for the intricate coordination of mitosis, septation, and cytokinesis (Simanis 2015). Similar to the homologous networks in animals, the kinase activity of SIN is inhibited by the SIN-inhibitory phosphatase complex, a homolog of STRIPAK (Singh *et al.* 2011). In filamentous fungi, this complex has already been extensively investigated (Kück *et al.* 2016), although detailed knowledge about STRIPAK-associated fungal kinases is still lacking. Further, interplay of STRIPAK and SIN has not yet been described for filamentous fungi. Recently, two GCKs—SmKIN3 and SmKIN24—from *Sordaria macrospora*, an ascomycete model organism, were reported as interaction partners of PRO11, the homolog of mammalian striatin (Frey *et al.* 2015). These authors further showed a high sequence similarity of SmKIN24 and SmKIN3 within their catalytic domains, and demonstrated that they are orthologs of the *Neurospora crassa* kinases MST-1 and septation initiation-deficient-1 (SID-1), respectively. The latter was previously shown to be part of SIN, the fungal counterpart of the mammalian Hippo pathway (Heilig *et al.* 2013; Frey *et al.* 2015).

Here, we investigate whether SmKIN3 links SIN with the STRIPAK complex. Therefore, we provide a detailed functional analysis of SmKIN3, using gene deletion and ATP-binding site variants of the SmKIN3 kinase. Further phenotypic analysis of single and double mutants was done to demonstrate a genetic interaction (GI) between SIN and the STRIPAK complex in filamentous fungi.

## Materials and Methods

### Strains, media, and growth conditions

All *S. macrospora* strains, as listed in Table 1, were grown under standard conditions (Nowrousian *et al.* 1999; Dirschnabel *et al.* 2014), unless otherwise described. Transformation of *S. macrospora* strains with recombinant plasmids was performed according to Nordziede *et al.* (2015), but without cyclase. Cloning was performed in *Saccharomyces cerevisiae* strain PJ69-4 $\alpha$  (James *et al.* 1996) using the homologous recombination

**Table 1 S. macrospora strains used in this study**

Strain	Relevant genotype	Relevant phenotype	Reference source
R19027	Wild-type, <i>sos1+</i>	F	Culture collection of the Department of General and Molecular Botany
S147487	Wild-type, <i>sos1-</i>	F	This study
S70823	<i>fus</i> , <i>sos1+</i>	F	Culture collection of the Department of General and Molecular Botany
S149233	<i>fus</i> , <i>sos1-</i>	F	This study
S96888	$\Delta ku70::nat^+$ , <i>sos1-</i>	F	Pöggeler and Kück (2006)
D2273	$\Delta Smkin3::hyg^+$ , <i>sos1-</i>	S, RS, HFD	This study
D2201	$\Delta Smkin3::hyg^+$ , <i>sos1+</i>	F	This study
D2387	$\Delta Smkin3::hyg^+/fus$ , <i>sos1-</i>	S, RS, HFD	This study
D2227	$\Delta Smkin3::hyg^+/fus$ , <i>sos1+</i>	F	This study
D2694	$\Delta Smkin3::hyg^+::Smkin3(p)::Smkin3::Smkin3(t)::nat^+$	F	This study
D2704	$\Delta Smkin3::hyg^+::gpd(p)::mrfp::Smkin3::trpC(t)::nat^+$	F, HS	This study
D2606	$\Delta Smkin3::hyg^+::Smkin3(p)::Smkin3^{K26R}::Smkin3(t)::nat^+$	F	This study
D160A-10	$\Delta Smkin3::hyg^+::Smkin3(p)::Smkin3^{K39R}::Smkin3(t)::nat^+$	S, NS, HFD, GD	This study
S63685	<i>pro11</i>	S, HFD	Pöggeler and Kück (2004)
S5.7	$\Delta pro11::hyg^+$	S, HFD	Bloemendal <i>et al.</i> (2012)
S141923	<i>pro11/fus</i>	S, HFD	Culture collection of the Department of General and Molecular Botany
$\Delta pro11/fus$	$\Delta pro11::hygr/fus$	S, HFD	Culture collection of the Department of General and Molecular Botany
S150712	$\Delta Smkin3::hyg^+/pro11$	S, NS, HFD	This study
S150772	$\Delta Smkin3::hyg^+/\Delta pro11::hyg^+$	S, NS, HFD	This study
S140253	$\Delta pro22::hyg^+/pro11$	S, HFD	This study
S140062	$\Delta pro22::hyg^+/\Delta pro11::hygr$	S, HFD	This study
S56	$\Delta pro22::hyg^+$	S, HFD	Bloemendal <i>et al.</i> (2012)
AB2854	$\Delta pro22::hyg^+::pro22::nat^+$	F	Beier (2017)

F, fertile; S, sterile; RS, rare septa; HFD, hyphal fusion defect; HS, hyperseptation; NS, no septa; GD, germination defect.

system described previously (Colot *et al.* 2006). For propagation of recombinant plasmids, *Escherichia coli* strains XL1-Blue MRF<sup>+</sup> (Jerpseth 1992) and NEB5 $\alpha$  (New England Biolabs, Beverly, MA) were used under standard conditions (Sambrook and Russell 2001).

### Generation of plasmids

All plasmids used in this study are listed in Table 2. To generate the knockout plasmid pKO4490 for the deletion of *Smkin3*, the yeast homologous recombination system was used. Yeast strain PJ69-4 $\alpha$  was transformed with two 1-kb PCR fragments carrying the 5' or 3' flanking sequences of *Smkin3*, respectively, together with a hygromycin B resistance cassette from pDrivehph and *EcoRI/XhoI*-linearized vector pRS426. Similarly, the yeast recombination system was used to obtain complementation plasmids pNAkin3 and pOEkin3.

To obtain pNAkin3, a 5.8-kb fragment carrying the *Smkin3* gene, together with 5' and 3' flanking regions and overlapping sequences for pRSnat, was amplified using 5'na4490-fw and 3'na4490-rv oligonucleotides (Table 3) from *S. macrospora* genomic DNA. The amplified fragment was recombined into *Bam*HI-linearized pRSnat.

pOEkin3 is a derivative of pDS23, in which the *egfp* gene was substituted by the *mrfp::Smkin3* fusion construct. Fragments of *mrfp* and *Smkin3*, with overlapping sequences to the *gpd* promoter and *trpC* terminator, were amplified with

oligonucleotides P<sub>gpd</sub>-*mrfp*-fw/*mrfp*-kin3-rv and *mrfp*-kin3-fw/kin3-T<sub>trpC</sub>-rv from pMHN2 and pNAkin3, respectively.

To generate point mutations in the *Smkin3* sequence encoding the ATP-binding site, we used the Q5 Site-Directed Mutagenesis Kit (New England Biolabs). Oligonucleotide pairs kin3K26R-Q5-fw/kin3K26R-Q5-rv and kin3K39R-Q5-2fw/kin3K39R-Q5-2rv were used. This resulted in plasmids p4490-K26R and p4490-K39R, which are both derivatives of pNAkin3, carrying A to G nucleotide substitution at positions 173 and 212 of the *Smkin3* gene, respectively.

### Generation and verification of *Smkin3* deletion strain and double-deletion mutants

To generate a  $\Delta Smkin3$  deletion strain, pKO4490 was linearized with *EcoRI*. The 3.4-kb  $\Delta Smkin3$  deletion cassette was transformed into  $\Delta ku70$  (Pöggeler and Kück 2006). The primary transformants were selected for hygromycin B resistance and verified by PCR. Ascospore isolates (AIs) of the  $\Delta Smkin3$  strain with the wild-type genetic background were obtained by crosses with the spore color mutant *fus1-1*, as described previously (Kück *et al.* 2009; Nowrousian *et al.* 2012), and verified by PCR and Southern Blot analysis (Supplemental Material, Figure S1).

For generation of  $\Delta Smkin3/pro11$  and  $\Delta Smkin3\Delta pro11$ , sterile *pro11/fus* and  $\Delta pro11/fus$  spore color mutants were crossed with the fertile black-spored complementation strain  $\Delta Smkin3::NAkin3$  (D2694). For generation of  $\Delta pro22/pro11$

**Table 2 Plasmids used in this study**

Plasmid	Feature	Reference
pRS426	<i>URA3, lacZ_a, bla</i>	Christianson <i>et al.</i> (1992)
pDrivehph	<i>trpC(p)::hph, lacZ_a, bla, kann</i>	Nowrousian and Cebula (2005)
pKO4490	Deletion cassette for <i>Smkin3</i> , 1 kb 5' flank, <i>hph</i> from pDrivehph and 1 kb 3' flank in pRS426	This study
pRSnat	<i>trpC(p)::nat, URA3, bla</i>	Klix <i>et al.</i> (2010)
pDS23	<i>gpd(p)::egfp::trpC(t), trpC(p)::nat, URA3, bla</i>	Schindler and Nowrousian (2014)
pMHN2	<i>gpd(p)::mrfp::trpC(t), trpC(p)::hph, bla</i>	Rech (2007)
pNAkin3	<i>Smkin3</i> with 1,9 kb upstream and 1,1 kb downstream sequence in pRSnat	This study
pOEkin3	<i>gpd(p)::mrfp::SmKin3::trpC(t)</i> in pRSnat	This study
p4490-K26R	pNAkin3 carrying <i>Smkin3</i> <sup>K26R</sup> mutation	This study
p4490-K39R	pNAkin3 carrying <i>Smkin3</i> <sup>K39R</sup> mutation	This study

and  $\Delta$ pro22 $\Delta$ pro11, pro11/fus and  $\Delta$ pro11/fus were crossed with the fertile black-spored complementation strain  $\Delta$ pro22komp (AB2854). Single spores were isolated from recombinant asci, and selected for hygromycin B resistance and nourseothricin sensitivity to outcross the complementation plasmid. Gene deletions were verified by PCR and Southern blot analysis (Figures S2 and S3). For verification of the pro11 point mutation, a 0.6-kb fragment was amplified with pro11mut-fw and pro11mut-rv oligonucleotides (Figure S2A), and sequenced with pro11mut-bw (data not shown).

### Microscopic investigations

Microscopic investigations were performed with an AxioImager microscope (Zeiss [Carl Zeiss], Thornwood, NY) equipped with a CoolSnap HQ camera (Roper Scientific) and a SpectraX LED lamp (Lumencor). Images were acquired and edited with MetaMorph (version 7.7.0.0; Universal Imaging).

To investigate sexual development by differential interference contrast microscopy, glass slides were covered with 5 ml solid malt–cornmeal fructification medium (BMM) and incubated for 2–7 days. Within this time period, different stages of fruiting body development can be observed (Engh *et al.* 2007; Teichert *et al.* 2014). The generation of ascogonia per square centimeter was examined after 3 days. Ascogonial coils were counted on BMM-coated glass slides ( $n = 4$ ), on the surface covered with a 22 × 32 mm coverslip.

Hyphal fusion assays were performed after 2 days of growth on minimal medium containing soluble starch overlaid with a cellophane layer (Bio-Rad, Hercules, CA) (Rech *et al.* 2007; Bloemendal *et al.* 2012).

Septa in vegetative mycelia and ascogonial coils were visualized by staining the cell wall with Calcofluor White M2R (CFW; Sigma [Sigma Chemical], St. Louis, MO), a 1,3- $\beta$ -glucan-binding agent (Roncero and Duran 1985). The 1  $\mu$ g/ml CFW stock solution was diluted 1:400 in a 0.9% NaCl solution and applied on 2-day-grown samples on BMM-coated glass slides, unless otherwise described. CFW fluorescence was analyzed using Chroma filter set 31000v2 (excitation filter D350/50, emission filter D460/50, and beam splitter 400 dclp; Chroma Technology, Bellows Falls, VT). The generation of septa per millimeter of hyphae was examined after 2 days of incubation on BMM-coated glass slides ( $n = 4$ ). In

each sample, one hypha was examined from the hyphal tip to the colony interior. Septa were quantified over the entire observed length (30 mm), including the bases of hyphal branches. For quantification of hyphal branch base septation, 100 branch bases were analyzed in two independent samples for each strain. Hyphal length measurements were taken in Adobe Photoshop.

### Phylogenetic analysis

Catalytic STK domain sequences were used as a base for the phylogenetic analysis. Multiple protein sequence alignments were performed using the ClustalW program (Larkin *et al.* 2007). The evolutionary history was inferred by using the maximum likelihood method (Jones *et al.* 1992). Obtained results were reproduced using the neighbor-joining method (Saitou and Nei 1987). To evaluate the statistical significance, a bootstrap analysis with 1000 iterations of bootstrap samplings was performed. Evolutionary analyses were conducted in MEGA7 (Kumar *et al.* 2016). The generated phylogenetic tree was exported to Adobe Illustrator and edited to optimize graphical representation.

### Data availability

Strains and plasmids are available upon request. The authors affirm that all data necessary for confirming the conclusions of the article are present within the article, figures, and tables. Supplemental material available at Figshare: <https://doi.org/10.25386/genetics.6741290>.

## Results

### GCKs from animals and fungi share highly homologous primary sequences

BLAST (basic local alignment search tool) analysis (Altschul *et al.* 1997) of full-length protein sequences confirms SmKIN3 as a homolog of SIN kinases Sid1p from *Sc. pombe*, SID-1 from *N. crassa*, and SEPL from *Aspergillus nidulans*, whereas no homologs were found in *Sa. cerevisiae*. In humans, there are 22 partially redundant GCKs described (Delpire 2009), while the *S. macrospora* genome carries only four genes for GCKs: SMAC\_04490 (*Smkin3*), SMAC\_01456

**Table 3 Oligonucleotides used in this study**

Oligonucleotide	Sequence (5'–3')	Specificity
KO-4490-5fw	gtaacgccagggtttccagtcacgacgaa ttcctccccatcgcgctaccaggata	<i>SmKin3</i> 5' flank with pRS426 overlap
KO-4490-5rv	cgagggcaaaggaatagggttccgtgagct tttggttacagaagggtgattgt	<i>SmKin3</i> 5' flank with <i>hph</i> overlap
KO-4490-3fw	gccccaaaatgctcctcaatcagttgctgag gtgatgaatggtgaagagaag	<i>hph</i> with <i>SmKin3</i> 3' flank overlap
KO-4490-3rv	gcgataacaatttcacacaggaacagcgaatt cctgttttggtactgtaacagccgt	<i>SmKin3</i> 3' flank with pRS426 overlap
SmKin3_F	atggccgacgaaggagtcgc	<i>SmKin3</i> start
SmKin3_R	ctaagatccggcaacagccc	<i>SmKin3</i> end
kin3- 5-2DR	aaccgtgtacttcgattggc	<i>SmKin3</i> 5' flank
kin3-3-DR2	aagcttgatcgccatggca	<i>SmKin3</i> 3' flank
hph1MN	cgatggctgtgtagaagtactcg	<i>hph</i>
hph2MN	atccgctggacgactaaaccaa	<i>hph</i>
5'na4490-fw	gacggatcgataagcttgatcgggtcctcaacggcgacctg	pRS426, <i>SmKin3</i> 5' UTR
3'na4490-rv	cgggcctctagaactagtgcaacagtaggta tgtacgtagctgc	<i>SmKin3</i> 3' UTR, pRS426
Pgpd-mrpf-fw	catcgagcttgactaacagctacatggcctcctcggaggagctcatc	<i>gpd(p)</i> , <i>mrpf</i>
mrpf-kin3-rv	gtcggccatagaaccaccaccggcgccg gtggagtggcg	<i>mrpf</i> , <i>SmKin3</i>
mrpf-kin3-fw	cgggccgggtggtggttctatggccgacgaaggagtcgccaac	<i>mrpf</i> , <i>SmKin3</i>
kin3-Ttrpc-rv	gtggatccactagtctagactaagatccggc aacagccccaccg	<i>SmKin3</i> , <i>trpc(t)</i>
kin3K26R-Q5-fw	cgtttacaggggaattgacagg	<i>SmKin3</i> K26 codon
kin3K26R-Q5-rv	acacaaaactgcctctgtg	<i>SmKin3</i> K26 codon
kin3K39R-Q5-2fw	gtggccatcagacatgtacg	<i>SmKin3</i> K39 codon
kin3K39R-Q5-2rv	tgtttcgcccgttgctctg	<i>SmKin3</i> K39 codon
pro11mut-fw	cgatgggaaagaggaaggg	<i>pro11</i> before <i>pro11</i> mutation
pro11mut-rv	cggggccttggtttgatc	<i>pro11</i> after <i>pro11</i> mutation
pro11-21	aagcgcgcttgccagtcgctgc	<i>pro11</i> 5' flank
pro11-kor	acgatcagcctcgaaagaccgc	<i>pro11</i> 3' flank
pro22- <i>Clal</i> -for	gcggggttttccagtatctacgattcatctgcagtaaccaaacattgag atcaaccacg	<i>pro22</i> gene
pro22- <i>SacI</i> -rv	cctccctagcagatgaggatgatgacatggttaaccattattggacctcaag accacgtg	<i>pro22</i> gene
pro22vp1	ccaagttcagcaacaagaggatgg	<i>pro22</i> 5' flank
pro22vp2	cttacggtagctacaaccctgata	<i>pro22</i> 3' flank

(*Smkin24*) (Frey *et al.* 2015), *SMAC\_04024* coding for the homolog of SEPH from *A. nidulans*, and *SMAC\_05827* coding for the homologs of Nak1p/Kic1p from *Sc. pombe* and *Sa. cerevisiae*, respectively. Protein sequence alignment shows that GCKs from different organisms are highly conserved only within the STK catalytic domain (amino acid positions 10–260 in *S. macrospora*). Therefore, an alignment of regions corresponding to this conserved domain (Figure S4) was used as a basis for the generation of a phylogenetic tree. As shown in Figure 1, maximum likelihood analysis of fungal GCKs and animal STRIPAK/Hippo-associated GCKs revealed the closest relationship between SmKIN3/SmKIN24 and the GCK-III subfamily, whereas the SEPH-like protein clade as well as the Nak1p/Kic1p homolog clade are more fungal-specific.

#### Generation and verification of a $\Delta$ *Smkin3* deletion strain

To functionally characterize SmKIN3, we generated a  $\Delta$ *Smkin3* deletion strain, as described in the *Materials and Methods* section. The *Smkin3* gene was substituted by a hygromycin B

resistance cassette (Figure S1) in the nonhomologous end-joining-deficient  $\Delta$ ku70 strain carrying a nourseothricin resistance marker gene. Primary transformants were able to grow on selection media containing both antibiotics. To outcross the  $\Delta$ ku70 deletion and to obtain homokaryotic  $\Delta$ *Smkin3* mutants,  $\Delta$ *Smkin3* $\Delta$ ku70 primary transformants were crossed with the brown-spored *fus1-1* mutant, which is fertile like the wild type (Nowrousian *et al.* 2012). Recombinant AIs were subsequently selected for hygromycin B resistance (*hyg*<sup>r</sup>) and nourseothricin sensitivity (*nat*<sup>s</sup>), which indicate a  $\Delta$ *Smkin3* genotype. Interestingly, some of the *hyg*<sup>r</sup> strains were sterile, while others were fertile, and thus able to develop wild-type-like mature fruiting bodies. PCR and Southern blot analysis showed that both sterile and fertile *hyg*<sup>r</sup> strains lacked the *Smkin3* gene (Figure S1).

We next crossed a sterile  $\Delta$ *Smkin3* (DR2273) to *fus1-1* and performed tetrad analysis. *Hyg*<sup>r</sup> strains corresponding to  $\Delta$ *Smkin3* and hygromycin B-sensitive (*hyg*<sup>s</sup>) strains corresponding to wild-type occurred with a ratio of  $\sim$ 1:1. As expected, all *hyg*<sup>s</sup> strains were fertile; however, the *hyg*<sup>r</sup>

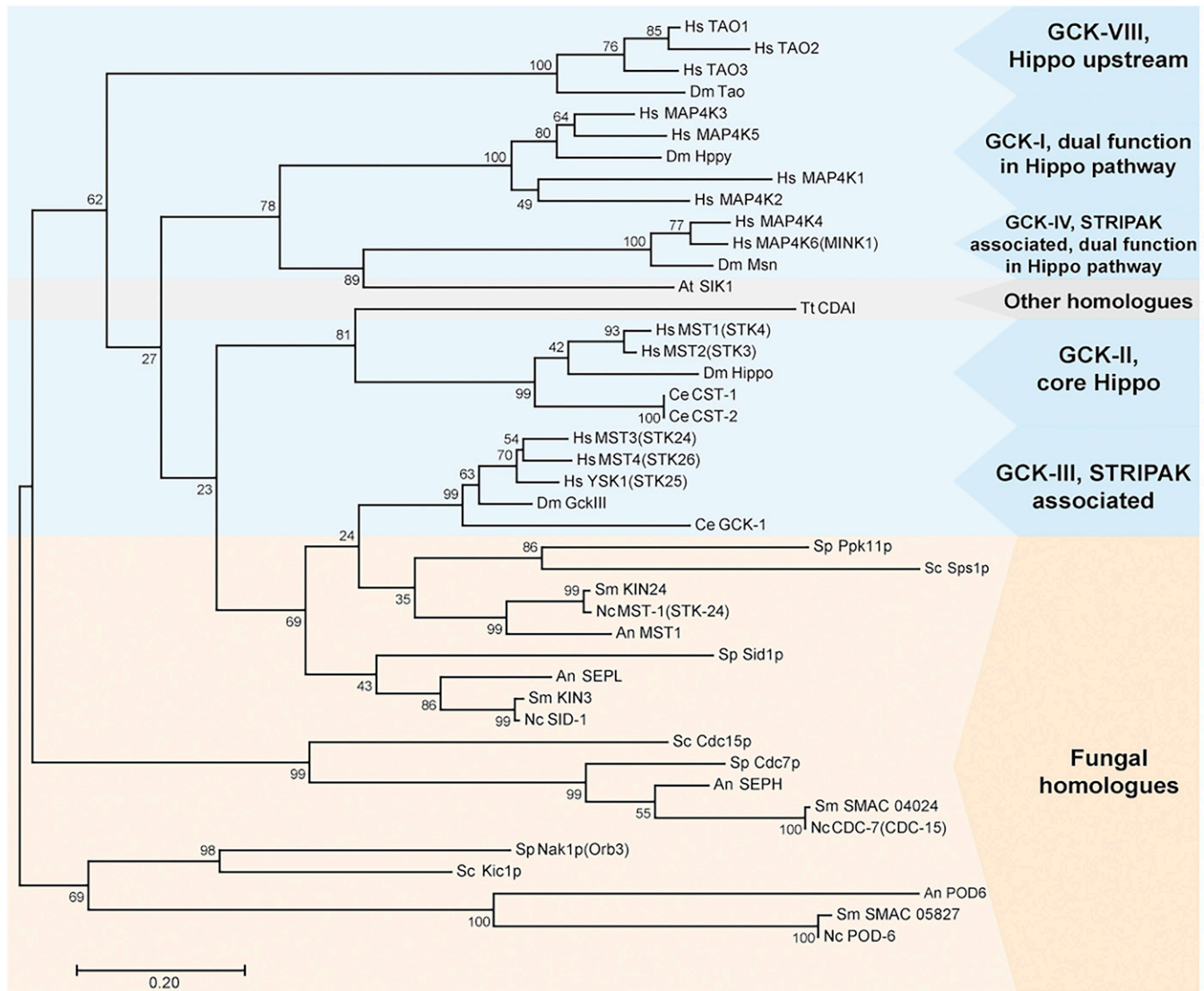


**Figure 1** Phylogenetic analysis of GCKs from animals (blue box), fungi (orange box), and plants and protozoans (gray box). Amino acid sequences were taken from the National Center for Biotechnology Information database. The phylogenetic tree was built using the maximum likelihood method based on the sequence alignment of conserved serine/threonine kinase domains from GCKs. The percentage of trees in which the associated taxa clustered together next to the branches ( $n = 1000$ ). An, *A. nidulans*; At, *Arabidopsis thaliana*; Dm, *D. melanogaster*; GCK, germinal center kinase; Hs, *Homo sapiens*; Nc, *N. crassa*; Sc, *Sa. cerevisiae*; Sm, *Sordaria macrospora*; Sp, *Sc. pombe*; STRIPAK, striatin-interacting phosphatases and kinases; Tt, *Tetrahymena thermophila*.

progeny showed a 1:1 ratio of fertile and sterile strains. This observation led to the hypothesis that an unknown genetic determinant rescued the developmental defect in the fertile  $\Delta\text{Smkin3}$  strains. We named this genetic determinant suppressor of sterility 1 (*sos1*). Accordingly, sterile and fertile  $\Delta\text{Smkin3}$  strains were designated  $\Delta\text{Smkin3}^{\text{sos1}-}$  and  $\Delta\text{Smkin3}^{\text{sos1}+}$ , respectively.

To further test the hypothesis of the presence of a suppressor, we performed tetrad analysis with different parental strains as detailed in Figure 2. Crosses of sterile  $\Delta\text{Smkin3}^{\text{sos1}-}$  with *fus1-1* produced *hyg<sup>s</sup>* fertile isolates corresponding to wild-type, as well as sterile and fertile *hyg<sup>r</sup>* isolates corresponding to  $\Delta\text{Smkin3}^{\text{sos1}-}$  and  $\Delta\text{Smkin3}^{\text{sos1}+}$ , respectively (Figure S5, cross 1). The  $\Delta\text{Smkin3}^{\text{sos1}-}:\Delta\text{Smkin3}^{\text{sos1}+}$  ratio

was  $\sim 1:1$ . In contrast, crosses of fertile  $\Delta\text{Smkin3}^{\text{sos1}+}$  with *fus1-1* produced wild-type isolates as well as fertile  $\Delta\text{Smkin3}^{\text{sos1}+}$ , but no sterile  $\Delta\text{Smkin3}^{\text{sos1}-}$  strains, indicating that *fus1-1* carries the *sos1+* allele (Figure S5, cross 2). To perform a cross in which both parental strains carry the *sos1-* allele, we obtained  $\text{wt}^{\text{sos1}-}$  strain S147487 from the cross of  $\Delta\text{Smkin3}^{\text{sos1}-}$  with *fus1-1*<sup>sos1+</sup> (Figure S5, cross 1). Strain S147487 was taken from a complete tetrad of this cross, in which all strains were fertile (Figure S5, cross 1), suggesting that the fertile  $\Delta\text{Smkin3}$  strains and not the wild-type strains carried the *sos1+* allele.  $\text{Wt}^{\text{sos1}-}$  was fertile and generated fruiting bodies like our laboratory wild-type strain, indicating that the suppressor mutation alone does not affect fruiting body development. Crossing sterile  $\Delta\text{Smkin3}^{\text{sos1}-}$  with

No	Cross	Ascus type				Quantitative spore analysis			
		P	T	R	nd	hyg <sup>S</sup>	hyg <sup>F</sup>	hyg <sup>S</sup> F	hyg <sup>S</sup> S
1	hyg <sup>S</sup> x ΔSmkin3 <sup>sos1-</sup> x wt <sup>sos1+</sup>	1	1	2	7	7	8	8	0
2	hyg <sup>F</sup> x ΔSmkin3 <sup>sos1+</sup> x wt <sup>sos1+</sup>	14	0	0	0	0	13	19	0
3	hyg <sup>S</sup> x ΔSmkin3 <sup>sos1-</sup> x wt <sup>sos1-</sup>	15	0	0	0	25	0	27	0
4	hyg <sup>F</sup> x ΔSmkin3 <sup>sos1+</sup> x wt <sup>sos1-</sup>	1	1	7	7	14	13	25	0

**Figure 2** Tetrad analysis to demonstrate the inheritance of the suppressor of sterility 1 (*sos1*) in *S. macrospora*. Sterile ( $\Delta\text{Smkin3}^{\text{sos1-}}$ , color code yellow) or fertile ( $\Delta\text{Smkin3}^{\text{sos1+}}$ , color code orange) deletion strains lacking *Smkin3* were crossed with wild-type (wt) strains carrying different alleles of *sos1* (S70823 wt<sup>sos1+</sup>, color code blue and S147487 wt<sup>sos1-</sup>, color code green). In all strains, we have neglected the *fus1-1* mutation since it is only a marker to recognize recombinant asci during ascospore isolation. Ascus type designation: P, parental; T, tetratype; R, recombinant; and nd, not determined due to a reduced spore germination. Phenotype designation: hyg<sup>S</sup>, hygromycin B-resistant, sterile ( $\Delta\text{Smkin3}^{\text{sos1-}}$ ); hyg<sup>F</sup>, hygromycin B-resistant, fertile ( $\Delta\text{Smkin3}^{\text{sos1+}}$ ); and hyg<sup>S</sup>F, hygromycin B-sensitive, fertile (wt<sup>sos1-</sup> and wt<sup>sos1+</sup>). Hyg<sup>S</sup> strains, which would indicate sterile wt strains, were never observed.

wt<sup>sos1-</sup> (S147487) generated only sterile  $\Delta\text{Smkin3}^{\text{sos1-}}$  and wild-type (Figure S5, cross 3), while crossing fertile  $\Delta\text{Smkin3}^{\text{sos1+}} \times \text{wt}^{\text{sos1-}}$  (S147487) resulted in a 1:1:2 distribution of sterile  $\Delta\text{Smkin3}^{\text{sos1-}}$ :fertile  $\Delta\text{Smkin3}^{\text{sos1+}}$ :wt (Figure 2 and Figure S5, cross 4). This result confirmed that *sos1* is a single gene that is inherited in a Mendelian manner independently from the *Smkin3* locus.

### The fungal *SmKIN3* kinase is involved in the septation and fusion of hyphae, as well as fruiting body formation

For further characterization, the  $\Delta\text{Smkin3}^{\text{sos1-}}$  strain was tested for septation and fusion of hyphae, as well as fruiting body formation. In parallel, the functional analysis of *SmKIN3* was completed by ectopic integration of the wild-type *Smkin3* gene in  $\Delta\text{Smkin3}^{\text{sos1-}}$ . In this analysis, two different complementation constructs were used with the *Smkin3* gene under the control of the weak native promoter, as known from RNA-sequencing data (Teichert *et al.* 2012), or a strong constitutive promoter (*gpd*) (Punt *et al.* 1992). The corresponding strains were designated  $\Delta\text{Smkin3}::\text{NAkin3}$  and  $\Delta\text{Smkin3}::\text{OEkin3}$ , respectively.

To examine the septation of vegetative mycelia, mycelium grown on rich medium was investigated microscopically after 16, 24, and 48 hr. We observed three different types of septa in this investigation: septa in trunk hyphae, in the base of branches, and in ascogonia (Figure 3A). As shown in Figure 3B, *S. macrospora* wild-type generated septa that were equally distributed over leading and branching hyphae. In contrast, the  $\Delta\text{Smkin3}^{\text{sos1-}}$  strain tended to form septa predominantly in the branch bases. These septa were visible directly after 16 hr of growth and the septation pattern remained constant after growth for  $\geq 2$  days. The septation defect was rescued by ectopic integration of complementation constructs, which is evident in Figure 3C. Strains carrying a construct with the native promoter ( $\Delta\text{Smkin3}::\text{NAkin3}$ )

showed a wild-type septation pattern, while the overexpression construct caused a hyperseptation phenotype in the bases of hyphal branches (Figure 3C). We quantified the hyperseptation phenotype (Figure 3D) as described in the *Materials and Methods* section. In  $\Delta\text{Smkin3}::\text{OEkin3}$ , two and three narrowly (2–12  $\mu\text{m}$  apart) spaced septa occurred in  $25 \pm 4\%$  and  $4 \pm 1\%$  of branches, respectively. In contrast, the wild-type and  $\Delta\text{Smkin3}::\text{NAkin3}$  strains generated double septa in hyphal branch bases only in  $5 \pm 2\%$  and  $5 \pm 0.5\%$  cases, respectively. In a total of 200 observed branches, we never found any triple septa.

Lack of STRIPAK subunits in *S. macrospora* leads to strictly correlating defects in the fusion of hyphae and fruiting body formation (Kück *et al.* 2016). Using light microscopy, we found that all  $\Delta\text{Smkin3}^{\text{sos1-}}$  strains have a hyphal fusion defect, which can be rescued by the ectopic integration of pNAkin3, but not pOEkin3 (Figure S6). Further, we analyzed the sexual development of the  $\Delta\text{Smkin3}^{\text{sos1-}}$  mutant and the two complementation strains. Unlike wild-type, the  $\Delta\text{Smkin3}^{\text{sos1-}}$  mutant forms aseptate female gametangia (ascogonia) and only a few immature unpigmented prefruiting bodies (properithecia) (Figure 4). Remarkably, ascogonial coils are extremely elongated, as was similarly observed in another sterile mutant *pro22* (Bloemendal *et al.* 2010). With both constructs, all complementation strains regained the fertile phenotype. Thus, generation of homokaryotic AIs was enabled via the isolation of ascospores from the selfing perithecia. Unlike the vegetative mycelium, ascogonia produced by the overexpressing strain did not visibly differ from those in the native expression strain with regard to the amount of septa and number of ascogonial coils.

### Functional analysis of double-mutant strains

Since *SmKIN3* was previously shown to interact with PRO11, the B<sup>'''</sup>-regulatory subunit of PP2A within STRIPAK (Frey

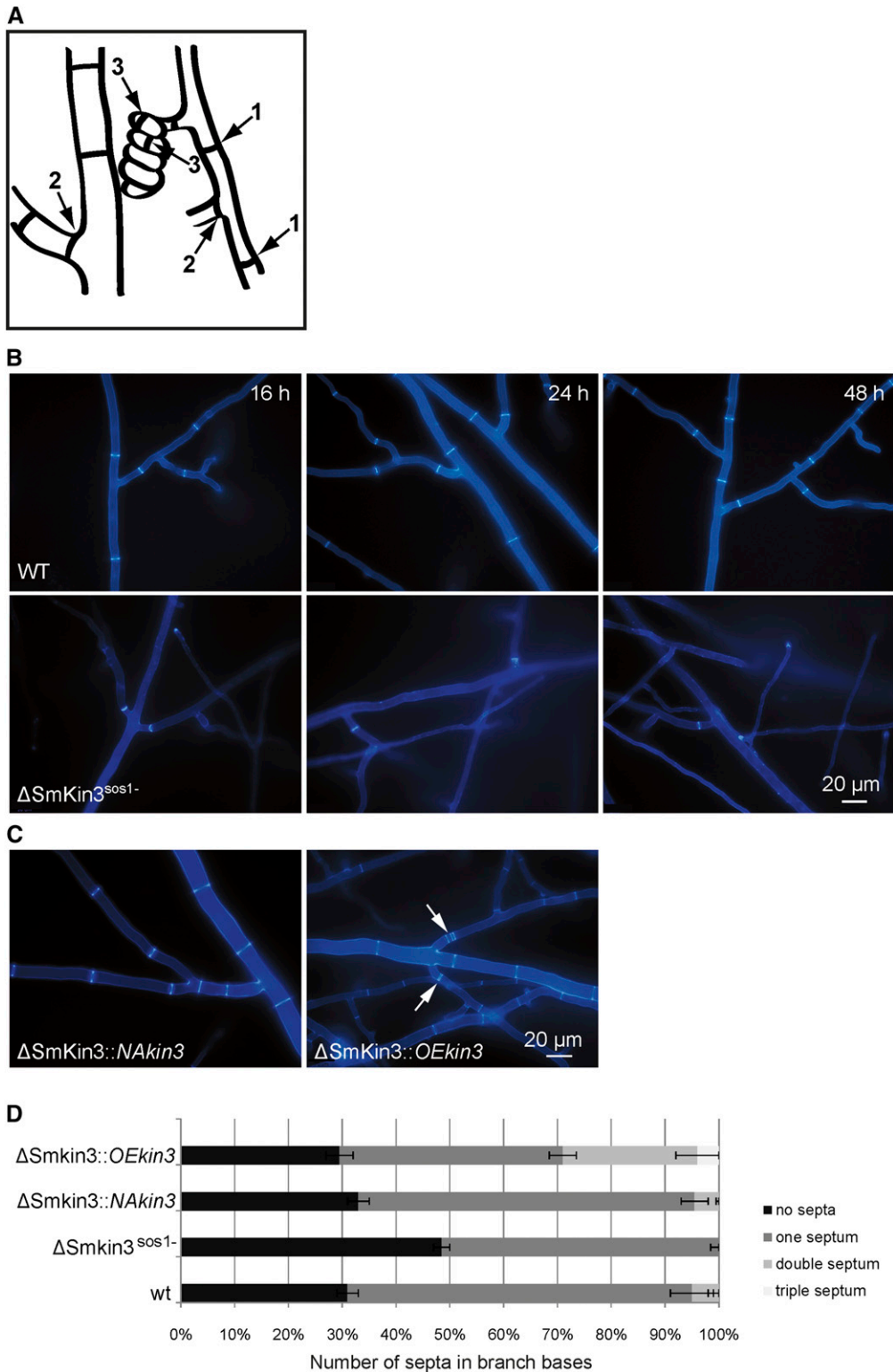


**Figure 3** Septation of the vegetative mycelium in wild-type (WT) and mutant strains as indicated. (A) Cartoon to indicate the three types of septa described in this investigation: septa in trunk hyphae (1), in the base of branches (2), and in ascogonia (3). (B) Septation in vegetative mycelium of the wild-type and  $\Delta SmKin3^{sos1-}$  strains after 16, 24, and 48 hr of incubation on BMM (solid malt–cornmeal fructification medium). (C) Complementation strains show WT-like hyphal septation.  $\Delta Smkin3::NAkin3$  and  $\Delta Smkin3::OEkin3$  indicate transformants, where fertility was restored by ectopic integration of the WT *Smkin3* gene under the control of a native (NA) or overexpression (OE) promoter. The arrows indicate multiple narrow-spaced septa in the strain overexpressing *Smkin3*. Mycelium samples were grown on BMM medium for 2 days and stained with Calcofluor White M2R. (D) Quantification of the hyperseptation phenotype in strains as indicated. Error bars show SD of two experiments ( $n = 100$ ).

*et al.* 2015), we generated double mutants  $\Delta Smkin3\Delta pro11$  and  $\Delta Smkin3/pro11$ .  $\Delta pro11$  was generated by genetic engineering and lacks the whole open reading frame for the PRO11 protein (Bloemendal *et al.* 2012), while the *pro11* mutant was discovered in a mutant screen and contains a stop codon at position 547. This results in a premature

translational termination of the open reading frame, and consequently *pro11* encodes only for the N-terminal part of the protein (Pöggeler and Kück 2004). We compared the morphology of both double mutants with the corresponding single mutants. Both double mutants showed distinct morphological features compared to either wild-type or single

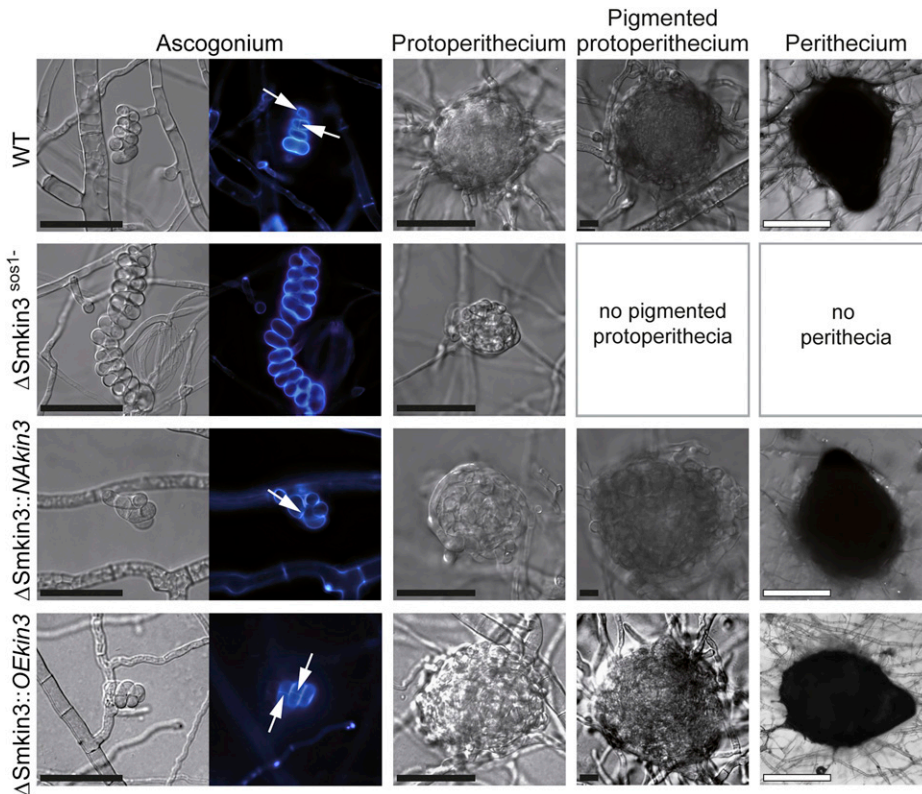


**Figure 4** Sexual development of wild-type (WT) and mutant strains. Strain denomination is the same as in Figure 2. Ascogonia, unpigmented and pigmented protoperithecia, as well as perithecia develop after 2, 3, 4, and 7 days, respectively, on complete solid malt–cornmeal fructification medium. Ascogonial coils were stained with Calcofluor White M2R and white arrows indicate septa. Bars: black represents 20  $\mu\text{m}$  and white represents 100  $\mu\text{m}$ .

mutants. Hyphal septation and fruiting body formation of the wild-type and  $\Delta\text{Smkin3}^{\text{sos1-}}$  strains was already shown in Figure 3 and Figure 4. As now seen in Figure 5, both *pro11* and  $\Delta\text{pro11}$  strains generate equally distributed septa in the vegetative mycelium, but only *pro11* is able to generate septa in ascogonial coils. This morphological difference is particularly remarkable since the truncated protein in *pro11* seems to be sufficient for regulating septum formation. On the other hand, both double mutants have completely aseptate mycelium and do not generate ascogonia at all. The severe septation defect renders both double mutants extremely sensitive to mechanical stress, so that any small damage causes complete leakage of hyphal contents (data not shown).

The observed changes in morphology were then quantified to chart the GI of *Smkin3* with *pro11*. GI refers to a double-mutant phenotype that is not easily explained by combining the effect of both single mutants. Negative GI results in severely compromised fitness and, in some cases, even synthetic lethality. In contrast, positive GI refers to a higher than expected fitness and a partial restoration of the wild-type phenotype. While negative GI usually occurs between members of different pathways, both of which regulate one essential biological process, positive GI can connect members of the same pathway (Costanzo *et al.* 2011; van Leeuwen *et al.* 2016). For the GI studies, double mutants  $\Delta\text{pro22}/\text{pro11}$  and  $\Delta\text{pro22}\Delta\text{pro11}$  served as controls. Both *PRO22* and *PRO11* belong to the core of the STRIPAK complex and interact physically with each other, a phenomenon that should be indicated by a positive interaction (Bloemendal *et al.* 2012). As depicted in Figure 6, ascogonia formation

per square centimeter as well as septum formation per millimeter in vegetative hyphae was used as the phenotypic readout to map the GI. From values obtained for single mutants, the expected fitness of the resultant double mutants ( $\Delta\text{Smkin3}/\text{pro11}$ ,  $\Delta\text{Smkin3}\Delta\text{pro11}$ ,  $\Delta\text{pro22}/\text{pro11}$ , and  $\Delta\text{pro22}\Delta\text{pro11}$ ) was calculated based on a multiplicative model (value double mutant = value mutant 1  $\times$  value mutant 2) (Costanzo *et al.* 2011). These expected values (light gray bars) were compared to the experimentally obtained values (Table 4). In the case of ascogonia formation, the absolute value for the *S. macrospora* wild-type is  $142.9 \pm 10.7$  ascogonia/cm<sup>2</sup>. The following values for mutant strains are relative to the wild-type, which was set to 1. The corresponding values for  $\Delta\text{Smkin3}$ ,  $\Delta\text{pro22}$ , *pro11*, and  $\Delta\text{pro11}$  are  $0.06 \pm 0.01$ ,  $0.77 \pm 0.06$ ,  $0.69 \pm 0.03$ , and  $0.05 \pm 0.02$ , respectively. From these data, the expected values for double mutants are as follows:  $\Delta\text{Smkin3}/\text{pro11}$ , 0.05 ( $0.06 \times 0.77$ );  $\Delta\text{Smkin3}\Delta\text{pro11}$ , 0.003 ( $0.06 \times 0.05$ );  $\Delta\text{pro22}/\text{pro11}$ , 0.53 ( $0.77 \times 0.69$ ); and  $\Delta\text{pro22}\Delta\text{pro11}$ , 0.04 ( $0.77 \times 0.05$ ). However, when we examined the ascogonia in the double mutants, we found significant deviations from the expected values. In detail,  $\Delta\text{Smkin3}/\text{pro11}$  and  $\Delta\text{Smkin3}\Delta\text{pro11}$  showed no ascogonium formation at all, while  $\Delta\text{pro22}/\text{pro11}$  ( $0.74 \pm 0.06$ ) and  $\Delta\text{pro22}\Delta\text{pro11}$  ( $0.05 \pm 0.006$ ), the two STRIPAK double mutants, had values that were significantly higher than expected (Figure 6A). Similar tendencies were found when septum formation per millimeter was taken as the phenotypic readout. The wild type generates  $19 \pm 1.9$  septa per millimeter vegetative mycelium, and this value was set to 1. The corresponding values for  $\Delta\text{Smkin3}$ ,  $\Delta\text{pro22}$ , *pro11*, and  $\Delta\text{pro11}$  were  $0.26 \pm 0.05$ ,  $0.96 \pm 0.11$ ,

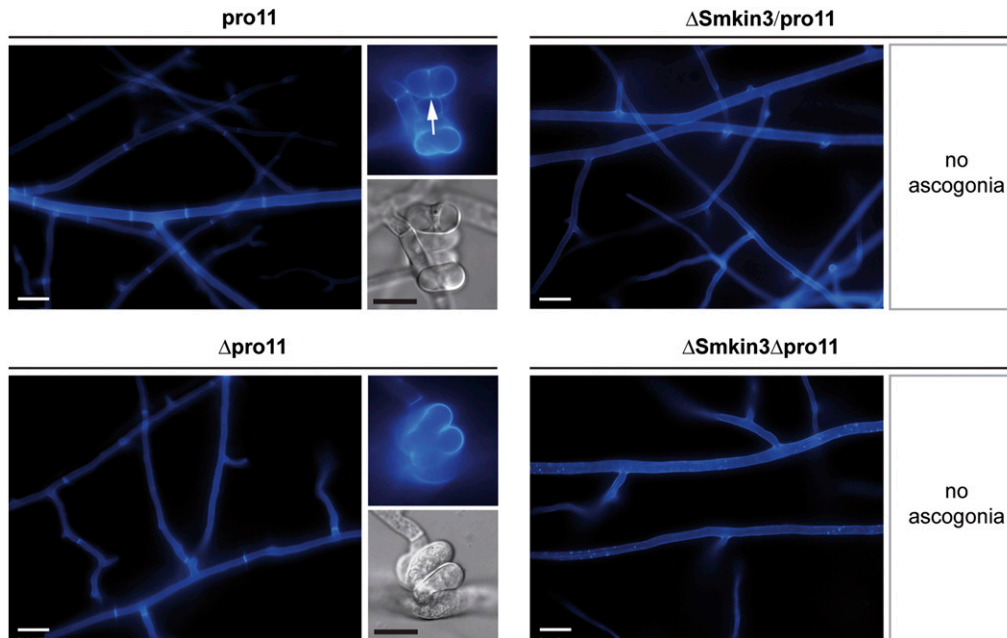


**Figure 5** Septation of the vegetative mycelium and ascogonial coils in *pro11* and  $\Delta pro11$  single mutants, as well as in  $\Delta Smkin3/pro11$  and  $\Delta Smkin3\Delta pro11$  double mutants. Arrow indicates septum in the ascogonial coil. Mycelium samples were grown on complete solid malt–cornmeal fructification medium for 2 days and stained with Calcofluor White M2R. Bars: white represent 20  $\mu m$  and black represent 10  $\mu m$ .

$0.94 \pm 0.12$ , and  $0.70 \pm 0.11$ , respectively. The expected values for the double mutants are 0.25 for  $\Delta Smkin3/pro11$ , 0.18 for  $\Delta Smkin3\Delta pro11$ , 0.91 for  $\Delta pro22/pro11$ , and 0.68 for  $\Delta pro22\Delta pro11$ . However, both *Smkin3* double mutants showed no septation at all. This negative deviation from the expected values has to be considered as negative GI, and according to Costanzo *et al.* (2011), these data point toward an interaction between members of different biological pathways. For the two STRIPAK double mutants ( $\Delta pro22/pro11$  and  $\Delta pro22\Delta pro11$ ), the experimentally obtained values ( $0.93 \pm 0.11$  and  $0.73 \pm 0.09$ ) did not significantly deviate from the expected ones (Figure 6B).

#### **A functional ATP-binding pocket of *SmKIN3* is required for fungal development**

Previous mutation analysis of conserved MST kinases showed that substitution of either of two conserved lysine residues by arginine residues results in variants lacking kinase activity *in vitro* (Lin *et al.* 2001; Huang *et al.* 2002). In an amino acid sequence alignment of *SmKIN3* with diverse MST kinases, we found that the abovementioned lysine residues are highly conserved and located within an ATP-binding pocket (Figure 7A). To investigate whether catalytic activity of *SmKIN3* is essential for its function in fungal development, we generated two single-point mutants at amino acid codons 26 or 39 of the *Smkin3* gene (*Smkin3*<sup>K26R</sup> and *Smkin3*<sup>K39R</sup>, respectively). These mutations result in lysine to arginine residue substitutions, which are depicted in Figure 7A. Ectopic integration of these mutant genes into  $\Delta Smkin3^{sos1-}$  resulted in recombinant strains, which were designated either  $\Delta Smkin3::kin3^{K26R}$  or  $\Delta Smkin3::kin3^{K39R}$ . As shown in Figure 7B,  $\Delta Smkin3::kin3^{K26R}$  was phenotypically similar to wild-type. However, transfer of *Smkin3*<sup>K39R</sup> into  $\Delta Smkin3^{sos1-}$  resulted in transformants with severe developmental defects,

clearly distinct from  $\Delta Smkin3^{sos1-}$  and more similar to  $\Delta Smkin3/pro11$  and  $\Delta Smkin3\Delta pro11$ . This result provides clear evidence for the requirement of *SmKIN3* kinase activity. To obtain homokaryotic AIs,  $\Delta Smkin3::kin3^{K39R}$  primary transformants were crossed with *fus1-1*. AIs from the recombinant perithecia were selected for nourseothricin resistance provided by a p4490-K39R plasmid. However, none of the isolated ascospores were able to grow on corresponding medium. Thus, we assume *Smkin3*<sup>K39R</sup> to be a dosage-dependent lethal mutation that cannot be tolerated in a homokaryotic background, but only in a heterokaryotic recipient one.

#### **Discussion**

Since the discovery of the first fungal striatin homolog PRO11 in *S. macrospora*, this fungus has been used as a model to study the related STRIPAK signaling complex (Pöggeler and Kück 2004; Bloemendal *et al.* 2012). The core of the STRIPAK complex is highly conserved and its architecture in *S. macrospora* resembles that in animals. PP2AA and PP2Ac1 are scaffolding and catalytic subunits of protein phosphatase 2A, respectively. PRO11 represents the B<sup>γ</sup>-regulatory subunit of PP2A that recruits a striatin-interacting protein 1/2 homolog PRO22, an SLMAP homolog PRO45, and a kinase activator SmMOB3 to the STRIPAK complex (Kück *et al.* 2016). *SmKIN3* and *SmKIN24* from *S. macrospora* were the first STRIPAK-associated GCKs ever described in fungi. They both were shown to interact directly with PRO11 (Frey *et al.* 2015), and our comparative sequence analysis reveals a phylogenetic relationship between *SmKIN3* and the GCK-III subfamily of striatin-associated kinases from animals. Further, *SmKIN3* is an ortholog of other characterized fungal SIN kinases, namely Sid1p from *Sc. pombe* and SEPL from

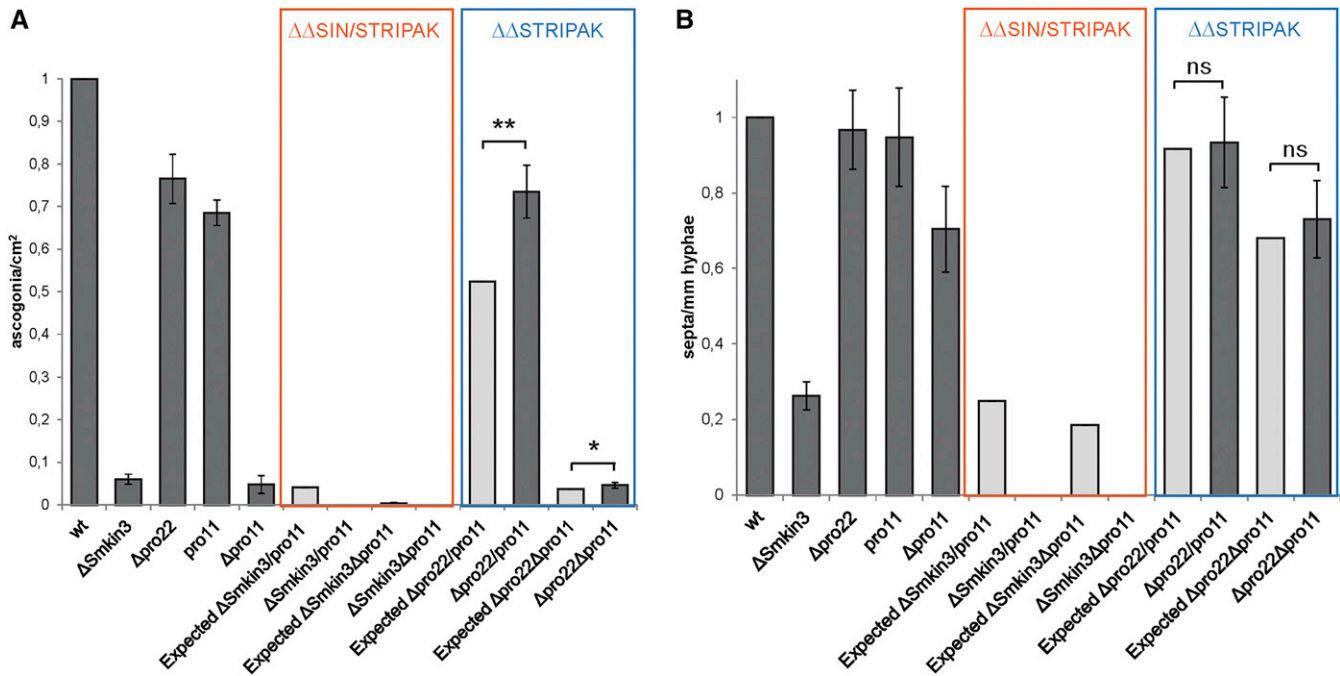


**Figure 6** Evaluation of the genetic interaction between SmKIN3 and PRO11 based on phenotypes of  $\Delta\text{Smkin3}/\text{pro11}$  and  $\Delta\text{Smkin3}\Delta\text{pro11}$  double mutants (orange frame).  $\Delta\text{pro22}/\text{pro11}$  and  $\Delta\text{pro22}\Delta\text{pro11}$  double mutants are taken as a control (blue frame). Dark gray bars indicate experimentally obtained values for single and double mutants; light gray bars indicate predicted values for double mutants based on single-mutant values (see *Results* for details). All values are given in relation to the wild-type (WT) absolute values, which are set to 1. For absolute values, see Table 4. Brackets indicate significant difference according to Student's *t*-test: \*  $P \leq 0.05$ ; \*\*  $P \leq 0.01$ ; and ns, not significant,  $P > 0.05$ . (A) Generation of ascogonia per square centimeter compared to WT. Samples were incubated for 3 days on solid malt–cornmeal fructification medium (BMM)-coated glass slides ( $n = 4$ ) (B) Generation of septa per millimeter hyphae compared to WT. Samples were incubated for 2 days on BMM-coated glass slides ( $n = 4$ ).

*A. nidulans*. From this, we predict SmKIN3 to be part of SIN. The phenotypic analysis of the  $\Delta\text{Smkin3}$  deletion mutant has shown a lack of septation, typical phenotypes of SIN mutants in other fungal systems. Thus, the role of SmKIN3 as a possible link between the fungal STRIPAK complex and SIN is very intriguing.

In this study, we provide detailed insight into SmKIN3 kinase function in diverse fungal developmental processes, such as septation and fusion of hyphae, as well as sexual propagation. Sterility, as well as hyphal fusion defects, are significant features already observed in diverse developmental mutants from *S. macrospora*, including those having a defect in STRIPAK subunits (Kück *et al.* 2016). Another feature, which was observed in  $\Delta\text{Smkin3}^{\text{sos1-}}$  and in some but not all STRIPAK mutants—namely *pro22*,  $\Delta\text{pro22}$ ,  $\Delta\text{pp2Ac1}$ , and  $\Delta\text{pro11}$  (Bloemendal *et al.* 2010; Beier *et al.* 2016, Figure 5)—is the generation of aseptate ascogonia. We have previously speculated that the lack of septa prevents the accumulation of signaling molecules, and thus, prevents further sexual development (Bloemendal *et al.* 2010). A further consequence of this developmental arrest may be the formation of overly elongated ascogonial coils, as observed in  $\Delta\text{pro22}$  and in this study for  $\Delta\text{Smkin3}^{\text{sos1-}}$  (Bloemendal *et al.* 2012). As described previously, protoperithecium development starts with the enveloping of an ascogonium with hyphae, which grow from ascogonium-bearing and adjacent hyphae (Mai 1976; Lord and Read 2011). We propose that mistargeting

of cell wall material and a defect of cell wall synthesis may initiate the extreme elongation of  $\Delta\text{Smkin3}^{\text{sos}}$  ascogonia instead of proper protoperithecium formation.

The phenotype described here for the  $\Delta\text{Smkin3}^{\text{sos1-}}$  mutant is significantly different from the *N. crassa* strain lacking the *Smkin3* homolog *sid-1*. Deletion of *sid-1* did not affect sexual propagation at all and triggered only a mild septation defect. Interestingly, the mutant strain generated aseptate hyphae after 18 hr of incubation, but after 36 hr, those reverted to the wild-type phenotype (Heilig *et al.* 2013). In contrast, the septation defect of  $\Delta\text{Smkin3}^{\text{sos1-}}$  is stable over a longer time interval, which indicates that SmKIN3 is a positive regulator of the septation process. Although there is high sequence similarity between catalytic domains from SmKIN24 and SmKIN3,  $\Delta\text{Smkin24}$  and  $\Delta\text{Smkin3}$  deletion strains have distinctly different phenotypes. Deletion of the *Smkin24* gene resulted in a developmental arrest at the late stage of the protoperithecium formation, as well as in the hyperseptation of the entire vegetative mycelium (Frey *et al.* 2015). This result led us to assume that both GCKs regulate septation in distinct ways in *S. macrospora*.

In *Sc. pombe*, GCK Sid1p was first discovered in a screen of *sid* temperature-sensitive mutants (Balasubramanian *et al.* 1998). The corresponding gene *sid1* is essential for viability, and strains lacking *sid1* fail to initiate medial ring constriction and septum formation. As a result, elongated multicellular cells are generated that will eventually lyse (Guertin *et al.*

**Table 4 Absolute values for verification of the genetic interactions**

Strain	Ascogonia/cm <sup>2</sup>	Septa/mm hyphae
Wild-type	142.9 ± 10.7	19.0 ± 1.9
ΔSmkin3	8.8 ± 1.7	5.0 ± 0.7
Δpro22	109.3 ± 8.2	18.4 ± 1.9
pro11	97.8 ± 4.2	18.0 ± 2.4
Δpro11	6.9 ± 3.0	13.4 ± 2.2
Expected ΔSmkin3/pro11	5.7	4.8
ΔSmkin3/pro11	0	0
Expected ΔSmkin3Δpro11	0.4	3.4
ΔSmkin3Δpro11	0	0
Expected Δpro22/pro11	74.7	17.3
Δpro22/pro11	105.0 ± 8.9	17.7 ± 2.2
Expected Δpro22Δpro11	5.2	12.9
Δpro22Δpro11	6.6 ± 0.9	13.9 ± 1.9

2000). Sid1p and homologous kinases in other fungi are responsible for septation and cytokinesis as a part of the conserved SIN. The SIN core in fission yeasts consists of GCK Sid1p with kinase adaptor Cdc14p and NDR kinase Sid2p, with a Mob1p kinase activator. This complex is similar to the mammalian MST1/2 and LATS1/2 GCK/NDR Hippo kinase cascade. In addition, fission yeasts and filamentous fungi possess an extra upstream GCK Cdc7p, which can activate Sid1p. Deletion and loss-of-function of SIN subunits in *Sc. pombe* causes the formation of elongated multicellular cells without septa. Moreover, overexpression, as well as deletion, of negative SIN regulators leads to a hyperseptation phenotype (Krapp and Simanis 2008; Simanis 2015). In our study, a similar effect was also observed for *S. macrospora*. SIN architecture in *N. crassa* is very similar to that of *Sc. pombe*. In *N. crassa*, GCK CDC-7 activates GCK SID-1, which in turn activates downstream NDR kinase DBF-2 (Heilig *et al.* 2013). Furthermore, MST-1, another GCK, has a dual function in activating two NDR kinases, namely DBF-2 in the SIN and COT-1 in the morphogenesis Orb6 (MOR) network (Seiler *et al.* 2006; Heilig *et al.* 2014). BLAST analysis revealed the presence of all putative SIN subunits in *S. macrospora*, wherein SmKIN3 is a homolog of SID-1 and SmKIN24 is a homolog of MST-1.

We previously observed that STRIPAK double mutant Δpp2Ac1Δpro22 has a phenotype that indicates only a slight reduction in fitness when compared with the corresponding single mutants. From this analysis, we concluded a positive GI of the corresponding genes (Beier *et al.* 2016). Here, we attained the same conclusion after analyzing Δpro22/pro11 and Δpro22Δpro11 mutants. However, the double mutants ΔSmkin3/pro11 and ΔSmkin3Δpro11 show a more severe defect than predicted. We consider this as indication of a negative GI, which can be explained when both SmKIN3 and PRO11 belong to different pathways and/or protein complexes. This assumption is consistent with data from *N. crassa*. There, it was shown that SID-1, the SmKIN3 homolog, is part of the SIN complex (Heilig *et al.* 2013). Our overall conclusion is that SmKIN3 is also a member of the SIN in *S. macrospora* and is connected with the STRIPAK complex by interacting with PRO11 (Frey *et al.* 2015).

The quantitative fitness analysis of double mutants has revealed clear indications of the negative GI of SIN subunit SmKIN3 and STRIPAK subunit PRO11, identifying their function in distinct biological pathways that are essential for septation and sexual development. However, the weak physical interaction between SmKIN3 and PRO11, demonstrated by Frey *et al.* (2015), hints toward the enzyme–substrate relationship. Whether PRO11 is a phosphorylation target of SmKIN3, or SmKIN3 is being recruited to the STRIPAK by PRO11 and dephosphorylated by PP2Ac, will be the subject of future studies.

To the best of our knowledge, this is the first study to provide *in vivo* evidence that GCK activity is essential for proper fungal cellular development, namely hyphal septation, fertility, and spore germination. Substitution of the conserved lysine 39 to arginine, which was predicted to alter the ATP-binding pocket of the kinase domain, resulted in a kinase-dead variation of SmKIN3. Moreover, since we never succeeded in isolating homokaryotic *Smkin3*<sup>K39R</sup> strains, *Smkin3*<sup>K39R</sup> seems to be a recessive lethal mutation. Thus, we propose that lethality is dependent on the dosage of the mutated protein SmKIN3<sup>K39R</sup> in the cell. We also propose that such a mutation is tolerated in dikaryotic primary transformants, which carry nuclei from the recipient. Due to ectopic integration of *Smkin3*<sup>K39R</sup> and its expression from the weak native promoter in some nuclei, the number of kinase-dead molecules remains low enough to enable viability of the fungus. Although the fitness of the recipient strain (ΔSmkin3<sup>Δ</sup>) is already reduced, the obtained transformants exhibit an even more reduced fitness. Expression of *Smkin3*<sup>K39R</sup> in all nuclei prevents basic survival functions, such as the germination of ascospores. An example of a point mutation that causes more severe developmental defects when compared to the complete deletion of the same gene is a phosphatase-dead mutant of PP2Ac1 in *S. macrospora*. Expression of the inactive phosphatase version in Δpp2Ac1 was not only unable to restore the developmental defect of the deletion strain, but also decreased its growth rate and the size of generated protoperithecia. However, the viability of AIs was not affected (Beier *et al.* 2016). We speculate that lack of SmKIN3 in the SIN signaling cascade is at least partially compensated by another kinase. A possible candidate is SmKIN24, since its *N. crassa* homolog MST-1 was previously shown to have an additional function in SIN (Heilig *et al.* 2014). Similarly, dual-function GCKs have been reported in animal systems. For example, STRIPAK-associated MAP4K4/6 in human and Hppy/Msn in fly are capable of Hippo pathway NDR kinase phosphorylation (Meng *et al.* 2015; Zheng *et al.* 2015). However, in *S. macrospora*, the physical presence of a kinase-dead SmKIN3 in a signaling cascade may prevent such a bypass. Indeed, kinase-dead SmKIN3 might bind all free target molecules, preventing interaction with an alternative activator (Figure 8).

In this study, we made the unexpected observation that dependent on the genetic background, fertility is restored in sterile ΔSmkin3 mutants. Moreover, we provide strong

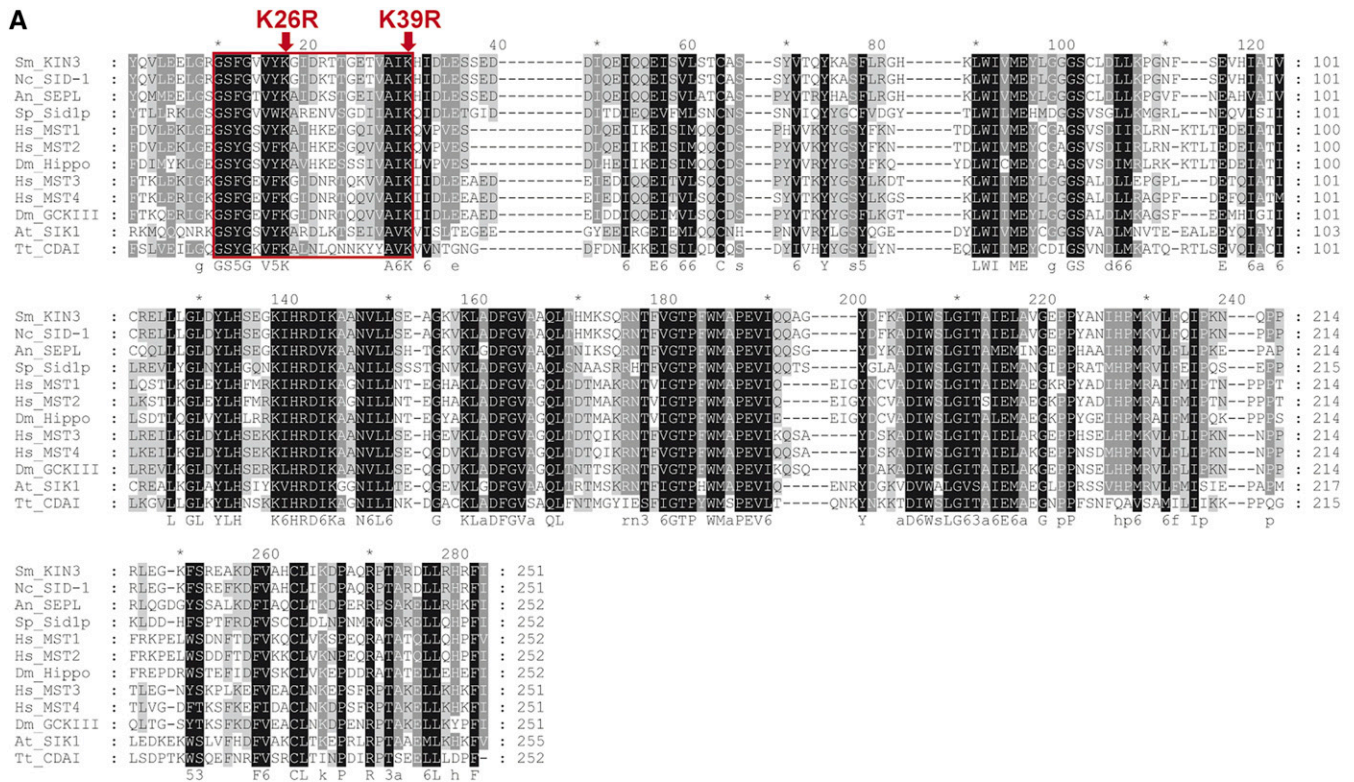


**Figure 7** Conserved lysine 39 within the ATP-binding pocket is essential for the biological function of SmKIN3. (A) Alignment of the conserved catalytic domains of SmKIN3 homologs from different organisms. The frame highlights the ATP-binding site. Two lysine to arginine substitutions of SmKIN3 are indicated by arrows. (B) Hyphal septation of transformants carrying either the K26R or K39R mutation, namely  $\Delta$ Smkin3::kin3<sup>K26R</sup> or  $\Delta$ Smkin3::kin3<sup>K39R</sup>, respectively. Mycelium samples were grown on solid malt-cornmeal fructification medium for 2 days and stained with Calcofluor White M2R. An, *A. nidulans*; At, *Arabidopsis thaliana*; Dm, *D. melanogaster*; Hs, *Homo sapiens*; Nc, *N. crassa*; Sc, *Sa. cerevisiae*; Sm, *Sordaria macrospora*; Sp, *Sc. pombe*; Tt, *Tetrahymena thermophila*.

evidence that a suppressor mutation derived from strain S70823 is responsible for this phenotype. Genetic suppression, as a particular case of a positive GI, occurs when a phenotype caused by a mutation in one gene is rescued by a mutation in another one (Costanzo *et al.* 2011; van Leeuwen *et al.* 2016). Mechanistic suppression classes, previously described in *Sa. cerevisiae*, are very diverse. Mutation within

one complex can be suppressed by the gain-of-function of another member of the same complex, whereas the loss-of-function of the negative regulator in the same pathway or a specific mutation would allow another protein to acquire a novel function and bypass the query mutation. In some rare cases, suppression can also be a result of alternative mRNA processing and protein degradation (van Leeuwen *et al.*

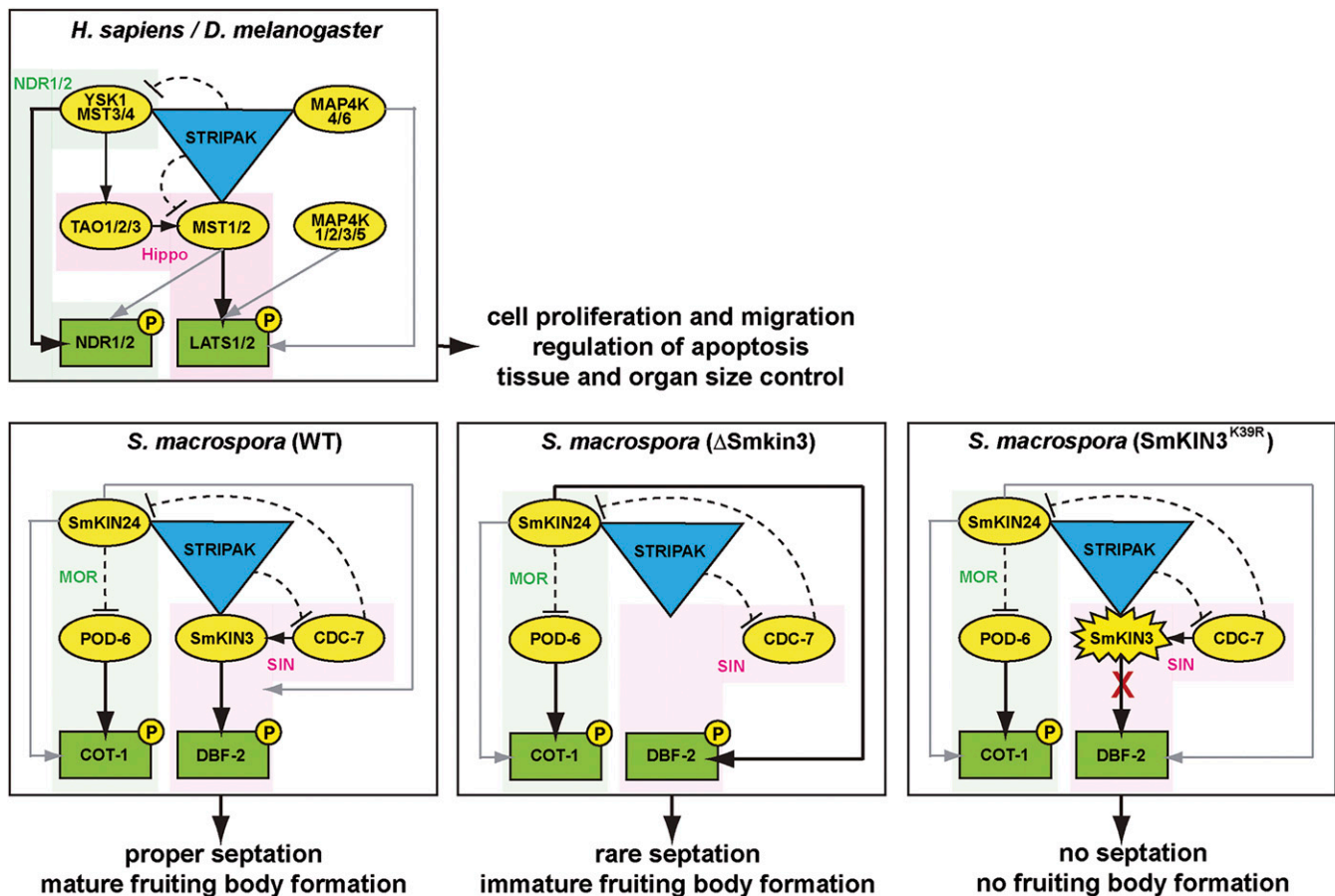


**Figure 8** Schematic representation of the GCK signaling network in animals and fungi. The animal model is generated based on the data obtained from the *H. sapiens* and *D. melanogaster* studies (referenced in the Introduction). The *S. macrospora* model is based on the data from *Sc. pombe* (Singh *et al.* 2011) and *N. crassa* (Heilig *et al.* 2013, 2014), as well as previous data from *S. macrospora* (Frey *et al.* 2015) and this study. STRIPAK corresponds to a striatin-interacting phosphatase and kinase complex. GCKs are represented as yellow ovals. NDR kinases are represented as green rectangles. Corresponding pathways are highlighted in green/pink. Solid black arrows indicate canonical kinase activation; solid gray arrows indicate optional bypass kinase activation; and dashed blunt-ended black lines indicate negative regulation. GCK, germinal center kinase; MOR, morphogenesis Orb6; NDR, nuclear Dbf2-related; SIN, septation initiation network; STRIPAK, striatin-interacting phosphatases and kinases.

2016). In the mitotic exit network (MEN), the homolog of the SIN from *Sa. cerevisiae*, multiple suppressor mutants are known as *telophase arrest bypassed (tab)*. One of the *tab* mutations results in gain-of-function of GCK Cdc15p, while other *tabs* are loss-of-function mutations in MEN negative regulators, such as GTPase-activating proteins Bub2p and Bfa1p, or PP2A subunits Cdc55p and Sit4p (Shou and Deshaies 2002). Similarly, a loss-of-function mutation in the Cdc55p homolog from *N. crassa* is suppressed by phosphomimetic mutations in COT-1, the NDR kinase of the MOR network (Shomin-Levi and Yarden 2017). In *A. nidulans*, loss-of-function mutations in genes coding for GCK SEPH and NDR kinase activator MOBA were suppressed by random mutations in five gene loci, called *suppressor of MobA (smo) A–E* (Kim *et al.* 2006). Further investigation of *smoA* and *smoB* revealed their putative function in a phosphoribosyl pyrophosphate synthesis pathway, whose function in the SIN remains ambiguous (Zhong *et al.* 2012). In the case of  $\Delta Smkin3^{sos1+}$ , we propose that *sos1* is a genetic suppressor of the phenotype caused by

the *Smkin3* deletion. Wherever the suppressor mutation might be located, its knowledge will improve our currently incomplete understanding of the architecture of eukaryotic signaling pathways and their regulation.

Finally, this study suggests that SmKIN3 links both the SIN and STRIPAK complex, thereby regulating multiple cellular processes. Further affinity chromatography studies combined with mass spectrometry analysis are currently underway to identify interaction partners of SmKIN3.

## Acknowledgments

We thank Susanne Schlewinski and Ingeborg Godehardt for their excellent technical assistance, Tim Dahlmann and Dominik Terfehr for their help in the bioinformatics analysis, M. Nowrousian for fruitful discussions, and G. Frenßen-Schenkel for assistance with graphical work. This work was funded by grants KU517/11-2, KU517/16-1, and PO523/4-2 from the Deutsche Forschungsgemeinschaft

(Bonn Bad-Godesberg, Germany). D.R. received a scholarship from the Friedrich-Ebert-Stiftung (Bonn, Germany).

## Literature Cited

- Altschul, S. F., T. L. Madden, A. A. Schäffer, J. Zhang, Z. Zhang *et al.*, 1997 Gapped BLAST and PSI-BLAST: a new generation of protein database search programs. *Nucleic Acids Res.* 25: 3389–3402. <https://doi.org/10.1093/nar/25.17.3389>
- Bae, S. J., L. Ni, A. Osinski, D. R. Tomchick, C. A. Brautigam *et al.*, 2017 SAV1 promotes Hippo kinase activation through antagonizing the PP2A phosphatase STRIPAK. *Elife* 6: e30278. <https://doi.org/10.7554/eLife.30278>
- Balasubramanian, M. K., D. McCollum, L. Chang, K. C. Wong, N. I. Naqvi *et al.*, 1998 Isolation and characterization of new fission yeast cytokinesis mutants. *Genetics* 149: 1265–1275.
- Beier, A., I. Teichert, C. Krisp, D. A. Wolters, and U. Kück, 2016 Catalytic subunit 1 of protein phosphatase 2A is a subunit of the STRIPAK complex and governs fungal sexual development. *MBio* 7: e00870-16. <https://doi.org/10.1128/mBio.00870-16>
- Beier, A. M., 2017 The STRIPAK-associated catalytic subunit 1 of protein phosphatase 2A governs sexual development in the filamentous fungus *Sordaria macrospora*. Dissertation, Ruhr-Universität Bochum, Germany.
- Bloemendal, S., K. M. Lord, C. Rech, B. Hoff, I. Engh *et al.*, 2010 A mutant defective in sexual development produces aseptate ascogonia. *Eukaryot. Cell* 9: 1856–1866. <https://doi.org/10.1128/EC.00186-10>
- Bloemendal, S., Y. Bernhards, K. Bartho, A. Dettmann, O. Voigt *et al.*, 2012 A homologue of the human STRIPAK complex controls sexual development in fungi. *Mol. Microbiol.* 84: 310–323. <https://doi.org/10.1111/j.1365-2958.2012.08024.x>
- Christianson, T. W., R. S. Sikorski, M. Dante, J. H. Shero, and P. Hieter, 1992 Multifunctional yeast high-copy-number shuttle vectors. *Gene* 110: 119–122. [https://doi.org/10.1016/0378-1119\(92\)90454-W](https://doi.org/10.1016/0378-1119(92)90454-W)
- Colot, H. V., G. Park, G. E. Turner, C. Ringelberg, C. M. Crew *et al.*, 2006 A high-throughput gene knockout procedure for *Neurospora* reveals functions for multiple transcription factors. *Proc. Natl. Acad. Sci. USA* 103: 10352–10357 (erratum: *Proc. Natl. Acad. Sci. USA* 103: 16614). <https://doi.org/10.1073/pnas.0601456103>
- Costanzo, M., A. Baryshnikova, C. L. Myers, B. Andrews, and C. Boone, 2011 Charting the genetic interaction map of a cell. *Curr. Opin. Biotechnol.* 22: 66–74. <https://doi.org/10.1016/j.copbio.2010.11.001>
- Couzens, A. L., J. D. Knight, M. J. Kean, G. Teo, A. Weiss *et al.*, 2013 Protein interaction network of the mammalian Hippo pathway reveals mechanisms of kinase-phosphatase interactions. *Sci. Signal.* 6: rs15. <https://doi.org/10.1126/scisignal.2004712>
- Delpire, E., 2009 The mammalian family of sterile 20p-like protein kinases. *Pflugers. Arch.* 458: 953–967. <https://doi.org/10.1007/s00424-009-0674-y>
- Dirschnabel, D. E., M. Nowrousian, N. Cano-Domínguez, J. Aguirre, I. Teichert *et al.*, 2014 New insights into the roles of NADPH oxidases in sexual development and ascospore germination in *Sordaria macrospora*. *Genetics* 196: 729–744. <https://doi.org/10.1534/genetics.113.159368>
- Engh, I., C. Würtz, K. Witzel-Schlömp, H. Y. Zhang, B. Hoff *et al.*, 2007 The WW domain protein PRO40 is required for fungal fertility and associates with Woronin bodies. *Eukaryot. Cell* 6: 831–843. <https://doi.org/10.1128/EC.00269-06>
- Fallahi, E., N. A. O'Driscoll, and D. Matallanas, 2016 The MST/Hippo pathway and cell death: a non-canonical affair. *Genes (Basel)* 7: 28. <https://doi.org/10.3390/genes7060028>
- Frey, S., E. J. Reschka, and S. Pöggeler, 2015 Germinal center kinases SmKIN3 and SmKIN24 are associated with the *Sordaria macrospora* striatin-interacting phosphatase and kinase (STRIPAK) complex. *PLoS One* 10: e0139163. <https://doi.org/10.1371/journal.pone.0139163>
- Glotzer, M., 2017 Cytokinesis in metazoa and fungi. *Cold Spring Harb. Perspect. Biol.* 9: a022343. <https://doi.org/10.1101/cshperspect.a022343>
- Gordon, J., J. Hwang, K. J. Carrier, C. A. Jones, Q. L. Kern *et al.*, 2011 Protein phosphatase 2a (PP2A) binds within the oligomerization domain of striatin and regulates the phosphorylation and activation of the mammalian Ste20-Like kinase Mst3. *BMC Biochem.* 12: 54. <https://doi.org/10.1186/1471-2091-12-54>
- Guertin, D. A., L. Chang, F. Irshad, K. L. Gould, and D. McCollum, 2000 The role of the sid1p kinase and cdc14p in regulating the onset of cytokinesis in fission yeast. *EMBO J.* 19: 1803–1815. <https://doi.org/10.1093/emboj/19.8.1803>
- Harvey, K. F., X. Zhang, and D. M. Thomas, 2013 The Hippo pathway and human cancer. *Nat. Rev. Cancer* 13: 246–257. <https://doi.org/10.1038/nrc3458>
- Heilig, Y., K. Schmitt, and S. Seiler, 2013 Phospho-regulation of the *Neurospora crassa* septation initiation network. *PLoS One* 8: e79464. <https://doi.org/10.1371/journal.pone.0079464>
- Heilig, Y., A. Dettmann, R. R. Mouriño-Pérez, K. Schmitt, O. Valerius *et al.*, 2014 Proper actin ring formation and septum constriction requires coordinated regulation of SIN and MOR pathways through the germinal centre kinase MST-1. *PLoS Genet.* 10: e1004306. <https://doi.org/10.1371/journal.pgen.1004306>
- Huang, C.-Y. F., Y.-M. Wu, C.-Y. Hsu, W.-S. Lee, M.-D. Lai *et al.*, 2002 Caspase activation of mammalian sterile 20-like kinase 3 (Mst3). Nuclear translocation and induction of apoptosis. *J. Biol. Chem.* 277: 34367–34374. <https://doi.org/10.1074/jbc.M202468200>
- Hwang, J., and D. C. Pallas, 2014 STRIPAK complexes: structure, biological function, and involvement in human diseases. *Int. J. Biochem. Cell Biol.* 47: 118–148. <https://doi.org/10.1016/j.biocel.2013.11.021>
- James, P., J. Halladay, and E. A. Craig, 1996 Genomic libraries and a host strain designed for highly efficient two-hybrid selection in yeast. *Genetics* 144: 1425–1436.
- Jerpseth, B., 1992 XL1-Blue MRF<sup>E</sup>. coli cells: McrA-, McrCB-, McrF-, Mrr-, HsdR-derivative of XL1-Blue cells. *Strategies* 5: 81–83.
- Johnson, R., and G. Halder, 2014 The two faces of Hippo: targeting the Hippo pathway for regenerative medicine and cancer treatment. *Nat. Rev. Drug Discov.* 13: 63–79. <https://doi.org/10.1038/nrd4161>
- Jones, D. T., W. R. Taylor, and J. M. Thornton, 1992 The rapid generation of mutation data matrices from protein sequences. *Bioinformatics* 8: 275–282. <https://doi.org/10.1093/bioinformatics/8.3.275>
- Kim, J.-M., L. Lu, R. Shao, J. Chin, and B. Liu, 2006 Isolation of mutations that bypass the requirement of the septation initiation network for septum formation and conidiation in *Aspergillus nidulans*. *Genetics* 173: 685–696. <https://doi.org/10.1534/genetics.105.054304>
- Klix, V., M. Nowrousian, C. Ringelberg, J. J. Loros, J. C. Dunlap *et al.*, 2010 Functional characterization of MAT1-1-specific mating-type genes in the homothallic ascomycete *Sordaria macrospora* provides new insights into essential and nonessential sexual regulators. *Eukaryot. Cell* 9: 894–905. <https://doi.org/10.1128/EC.00019-10>
- Krapp, A., and V. Simanis, 2008 *An Overview of the Fission Yeast Septation Initiation Network (SIN)*. Portland Press Limited, London.
- Kück, U., S. Pöggeler, M. Nowrousian, N. Nolting, and I. Engh, 2009 *Sordaria macrospora*, a model system for fungal

- development pp. 17–39 in *Physiology and Genetics, The Mycota XV*. Springer, Berlin. [https://doi.org/10.1007/978-3-642-00286-1\\_2](https://doi.org/10.1007/978-3-642-00286-1_2)
- Kück, U., A. M. Beier, and I. Teichert, 2016 The composition and function of the striatin-interacting phosphatases and kinases (STRIPAK) complex in fungi. *Fungal Genet. Biol.* 90: 31–38. <https://doi.org/10.1016/j.fgb.2015.10.001>
- Kumar, S., G. Stecher, and K. Tamura, 2016 MEGA7: molecular evolutionary genetics analysis version 7.0 for bigger datasets. *Mol. Biol. Evol.* 33: 1870–1874. <https://doi.org/10.1093/molbev/msw054>
- Larkin, M. A., G. Blackshields, N. P. Brown, R. Chenna, P. A. McGettigan *et al.*, 2007 Clustal W and Clustal X version 2.0. *Bioinformatics* 23: 2947–2948. <https://doi.org/10.1093/bioinformatics/btm404>
- Li, S., Y. S. Cho, T. Yue, Y. T. Ip, and J. Jiang, 2015 Overlapping functions of the MAP4K family kinases Hppy and Msn in Hippo signaling. *Cell Discov.* 1: 15038. <https://doi.org/10.1038/celldisc.2015.38>
- Lin, J.-L., H.-C. Chen, H.-I. Fang, D. Robinson, H.-J. Kung *et al.*, 2001 MST4, a new Ste20-related kinase that mediates cell growth and transformation via modulating ERK pathway. *Oncogene* 20: 6559–6569. <https://doi.org/10.1038/sj.onc.1204818>
- Lord, K. M., and N. D. Read, 2011 Perithecial morphogenesis in *Sordaria macrospora*. *Fungal Genet. Biol.* 48: 388–399. <https://doi.org/10.1016/j.fgb.2010.11.009>
- Madsen, C. D., S. Hooper, M. Tozluoglu, A. Bruckbauer, G. Fletcher *et al.*, 2015 STRIPAK components determine mode of cancer cell migration and metastasis. *Nat. Cell Biol.* 17: 68–80. <https://doi.org/10.1038/ncb3083>
- Mai, S. H., 1976 Morphological studies in *Podospira anserina*. *Am. J. Bot.* 63: 821–825. <https://doi.org/10.1002/j.1537-2197.1976.tb11871.x>
- Maugeri-Saccà, M., and R. De Maria, 2018 The Hippo pathway in normal development and cancer. *Pharmacol. Ther.* 186: 60–72. <https://doi.org/10.1016/j.pharmthera.2017.12.011>
- Meng, Z., T. Moroishi, V. Mottier-Pavie, S. W. Plouffe, C. G. Hansen *et al.*, 2015 MAP4K family kinases act in parallel to MST1/2 to activate LATS1/2 in the Hippo pathway. *Nat. Commun.* 6: 8357. <https://doi.org/10.1038/ncomms9357>
- Meng, Z., T. Moroishi, and K.-L. Guan, 2016 Mechanisms of Hippo pathway regulation. *Genes Dev.* 30: 1–17. <https://doi.org/10.1101/gad.274027.115>
- Nordzike, S., T. Zobel, B. Fränzel, D. A. Wolters, U. Kück *et al.*, 2015 A fungal sarcolemmal membrane-associated protein (SLMAP) homolog plays a fundamental role in development and localizes to the nuclear envelope, endoplasmic reticulum, and mitochondria. *Eukaryot. Cell* 14: 345–358. <https://doi.org/10.1128/EC.00241-14>
- Nowrousian, M., and P. Cebula, 2005 The gene for a lectin-like protein is transcriptionally activated during sexual development, but is not essential for fruiting body formation in the filamentous fungus *Sordaria macrospora*. *BMC Microbiol.* 5: 64. <https://doi.org/10.1186/1471-2180-5-64>
- Nowrousian, M., S. Masloff, S. Pöggeler, and U. Kück, 1999 Cell differentiation during sexual development of the fungus *Sordaria macrospora* requires ATP citrate lyase activity. *Mol. Cell. Biol.* 19: 450–460. <https://doi.org/10.1128/MCB.19.1.450>
- Nowrousian, M., I. Teichert, S. Masloff, and U. Kück, 2012 Whole-genome sequencing of *Sordaria macrospora* mutants identifies developmental genes. *G3 (Bethesda)* 2: 261–270. <https://doi.org/10.1534/g3.111.001479>
- Pan, D., 2007 Hippo signaling in organ size control. *Genes Dev.* 21: 886–897. <https://doi.org/10.1101/gad.1536007>
- Pan, D., 2010 The hippo signaling pathway in development and cancer. *Dev. Cell* 19: 491–505. <https://doi.org/10.1016/j.devcel.2010.09.011>
- Pöggeler, S., and U. Kück, 2004 A WD40 repeat protein regulates fungal cell differentiation and can be replaced functionally by the mammalian homologue striatin. *Eukaryot. Cell* 3: 232–240. <https://doi.org/10.1128/EC.3.1.232-240.2004>
- Pöggeler, S., and U. Kück, 2006 Highly efficient generation of signal transduction knockout mutants using a fungal strain deficient in the mammalian ku70 ortholog. *Gene* 378: 1–10. <https://doi.org/10.1016/j.gene.2006.03.020>
- Punt, P. J., C. Kramer, A. Kuyvenhoven, P. H. Pouwels, and C. A. van den Hondel, 1992 An upstream activating sequence from the *Aspergillus nidulans* gpdA gene. *Gene* 120: 67–73. [https://doi.org/10.1016/0378-1119\(92\)90010-M](https://doi.org/10.1016/0378-1119(92)90010-M)
- Rech, C., 2007 Molekulargenetische Charakterisierung des pro22-Gens aus *Sordaria macrospora*: die funktionelle Beteiligung von PRO22 an der Zelldifferenzierung bei Ascomyceten. Dissertation, Ruhr-Universität Bochum, Germany
- Rech, C., I. Engh, and U. Kück, 2007 Detection of hyphal fusion in filamentous fungi using differently fluorescence-labeled histones. *Curr. Genet.* 52: 259–266. <https://doi.org/10.1007/s00294-007-0158-6>
- Ribeiro, P. S., F. Josué, A. Wepf, M. C. Wehr, O. Rinner *et al.*, 2010 Combined functional genomic and proteomic approaches identify a PP2A complex as a negative regulator of Hippo signaling. *Mol. Cell* 39: 521–534. <https://doi.org/10.1016/j.molcel.2010.08.002>
- Richardson, H. E., and M. Portela, 2017 Tissue growth and tumorigenesis in *Drosophila*: cell polarity and the Hippo pathway. *Curr. Opin. Cell Biol.* 48: 1–9. <https://doi.org/10.1016/j.ceb.2017.03.006>
- Roncero, C., and A. Duran, 1985 Effect of Calcofluor white and Congo red on fungal cell wall morphogenesis: in vivo activation of chitin polymerization. *J. Bacteriol.* 163: 1180–1185.
- Saitou, N., and M. Nei, 1987 The neighbor-joining method: a new method for reconstructing phylogenetic trees. *Mol. Biol. Evol.* 4: 406–425. <https://doi.org/10.1093/oxfordjournals.molbev.a040454>
- Sambrook, J., and D. W. Russell, 2001 *Molecular Cloning: A Laboratory Manual*, Ed. 3. Cold Spring Harbor Laboratory Press, Cold Spring Harbor, NY.
- Schindler, D., and M. Nowrousian, 2014 The polyketide synthase gene pks4 is essential for sexual development and regulates fruiting body morphology in *Sordaria macrospora*. *Fungal Genet. Biol.* 68: 48–59. <https://doi.org/10.1016/j.fgb.2014.04.008>
- Sebé-Pedrós, A., Y. Zheng, I. Ruiz-Trillo, and D. Pan, 2012 Premetazoan origin of the hippo signaling pathway. *Cell Rep.* 1: 13–20. <https://doi.org/10.1016/j.celrep.2011.11.004>
- Sebé-Pedrós, A., M. I. Peña, S. Capella-Gutiérrez, M. Antó, T. Gabaldón *et al.*, 2016 High-throughput proteomics reveals the unicellular roots of animal phosphosignaling and cell differentiation. *Dev. Cell* 39: 186–197. <https://doi.org/10.1016/j.devcel.2016.09.019>
- Seiler, S., N. Vogt, C. Ziv, R. Gorovits, and O. Yarden, 2006 The STE20/germinal center kinase POD6 interacts with the NDR kinase COT1 and is involved in polar tip extension in *Neurospora crassa*. *Mol. Biol. Cell* 17: 4080–4092. <https://doi.org/10.1091/mbc.e06-01-0072>
- Shomin-Levi, H., and O. Yarden, 2017 The *Neurospora crassa* PP2A regulatory subunits RGB1 and B56 are required for proper growth and development and interact with the NDR kinase COT1. *Front. Microbiol.* 8: 1694. <https://doi.org/10.3389/fmicb.2017.01694>
- Shou, W., and R. J. Deshaies, 2002 Multiple telophase arrest bypassed (tab) mutants alleviate the essential requirement for Cdc15 in exit from mitosis in *S. cerevisiae*. *BMC Genet.* 3: 4. <https://doi.org/10.1186/1471-2156-3-4>
- Simanis, V., 2015 Pombe's thirteen-control of fission yeast cell division by the septation initiation network. *J. Cell Sci.* 128: 1465–1474. <https://doi.org/10.1242/jcs.094821>
- Singh, N. S., N. Shao, J. R. McLean, M. Sevugan, L. Ren *et al.*, 2011 SIN-inhibitory phosphatase complex promotes Cdc11p

- dephosphorylation and propagates SIN asymmetry in fission yeast. *Curr. Biol.* 21: 1968–1978. <https://doi.org/10.1016/j.cub.2011.10.051>
- Teichert, I., G. Wolff, U. Kück, and M. Nowrousian, 2012 Combining laser microdissection and RNA-seq to chart the transcriptional landscape of fungal development. *BMC Genomics* 13: 511. <https://doi.org/10.1186/1471-2164-13-511>
- Teichert, I., M. Nowrousian, S. Pöggeler, and U. Kück, 2014 The filamentous fungus *Sordaria macrospora* as a genetic model to study fruiting body development. *Adv. Genet.* 87: 199–244. <https://doi.org/10.1016/B978-0-12-800149-3.00004-4>
- Thompson, B. J., and E. Sahai, 2015 MST kinases in development and disease. *J. Cell Biol.* 210: 871–882. <https://doi.org/10.1083/jcb.201507005>
- Xiang, L., H. Yu, X. Zhang, B. Wang, Y. Yuan *et al.*, 2018 The versatile hippo pathway in oral-maxillofacial development and bone remodeling. *Dev. Biol.* 440: 53–63. <https://doi.org/10.1016/j.ydbio.2018.05.017>
- van Leeuwen, J., C. Pons, J. C. Mellor, T. N. Yamaguchi, H. Friesen *et al.*, 2016 Exploring genetic suppression interactions on a global scale. *Science* 354: aag0839. <https://doi.org/10.1126/science.aag0839>
- Yin, H., Z. Shi, S. Jiao, C. Chen, W. Wang *et al.*, 2012 Germinal center kinases in immune regulation. *Cell. Mol. Immunol.* 9: 439–445. <https://doi.org/10.1038/cmi.2012.30>
- Zheng, Y., W. Wang, B. Liu, H. Deng, E. Uster *et al.*, 2015 Identification of Happyhour/MAP4K as alternative Hpo/Mst-like kinases in the Hippo kinase cascade. *Dev. Cell* 34: 642–655. <https://doi.org/10.1016/j.devcel.2015.08.014>
- Zhong, G., W. Wei, Q. Guan, Z. Ma, H. Wei *et al.*, 2012 Phosphoribosyl pyrophosphate synthetase, as a suppressor of the sepH mutation in *Aspergillus nidulans*, is required for the proper timing of septation. *Mol. Microbiol.* 86: 894–907. <https://doi.org/10.1111/mmi.12026>

Communicating editor: A. Gladfelter